

# Biomimetic apatite nanocrystals: overview of their preparation, characterization and applications

**Dr. Michele Iafisco**

**[michele.iafisco@istec.cnr.it](mailto:michele.iafisco@istec.cnr.it)**

Laboratory of Bioceramics and Bio-hybrid Composites, CNR-Institute of Science and Technology for Ceramics (ISTEC), Via Granarolo, 64 48018 Faenza, ITALY



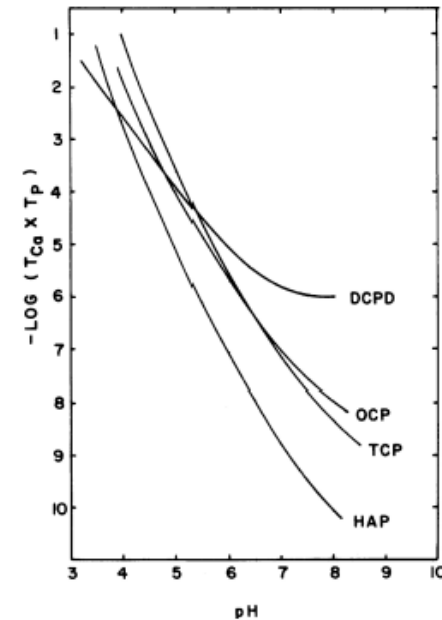
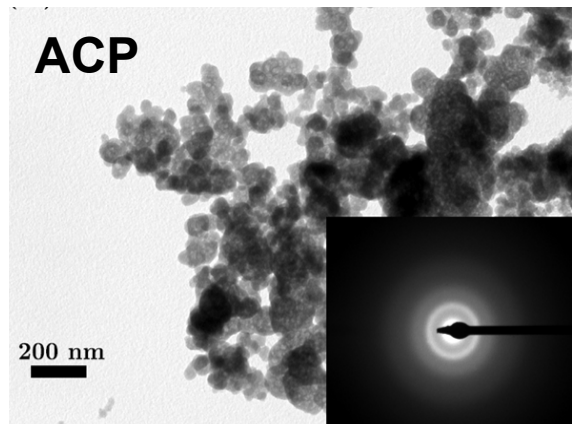
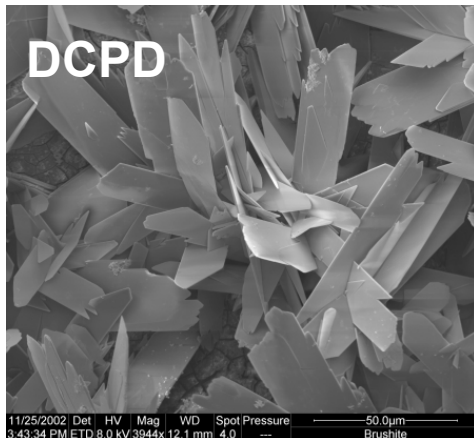
# Table of contents

- **Introduction**
- **Apatite Nanocrystals: Crystallization and characterization**
  - Batch crystallization
  - Sitting drop vapour diffusion
  - Thermal decomplexing method
- **Applications**
  - Organic-Inorganic Composites (Micro-nanospheres)
  - Coatings
  - Drug Delivery Systems

# Calcium phosphate phases

Ca/P	Compound	Formula
1.00	Dicalcium Phosphate, DCPD	$CaHPO_4 \cdot 2H_2O$
1.33	Octacalcium Phosphate, OCP	$Ca_8(HPO_4)_2(PO_4)_4 \cdot 5H_2O$
1.20-2.20	Amorphous Calcium Phosphate, ACP	$Ca_x H_y (PO_4)_z \cdot nH_2O$
1.50	Tricalcium Phosphate, TCP	$Ca_3(PO_4)_2$
1.67	Hydroxyapatite, HAP	$Ca_5(PO_4)_3(OH)$

The stability depends on the pH, ionic strength and temperature



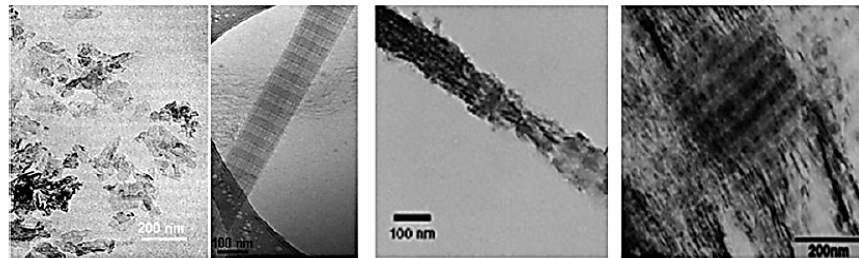
Wang and Nancollas, *Chem Rev*, 2008

Gomez-Morales et al., *Prog Cryst Growth Charact Mater*, 2013

Solubility isotherms of CaP phases at 37 °C and I=0.1 M

# Hydroxyapatite

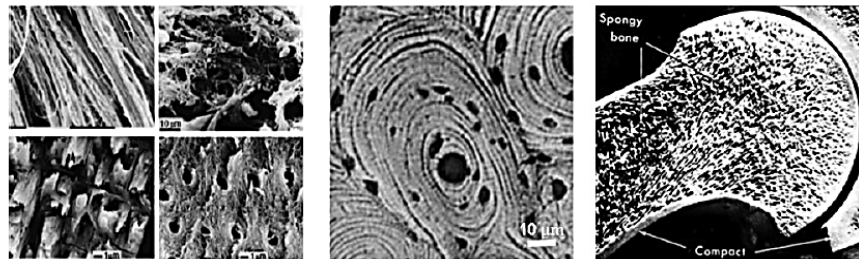
Hydroxyapatite is the main mineral component in bone, dentin and enamel



Level 1: Major components

Level 2: Mineralized Collagen

Level 3: Fibril Array



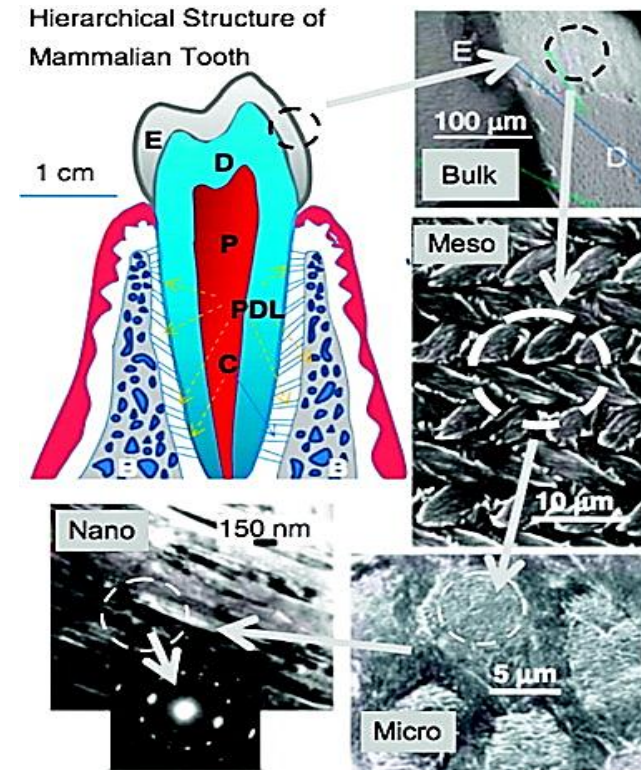
Level 4: Fibril Array Patterns

Level 5: Osteons

Level 6: Spongy vs Compact Bone



Level 7: Whole Bone



**Apatites with improved similarities with the biological ones can display better biological performances than coarser crystals**

Weiner and Wagner, *Annu Rev Mater Sci*, 1998

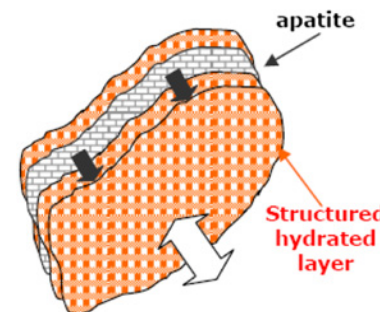
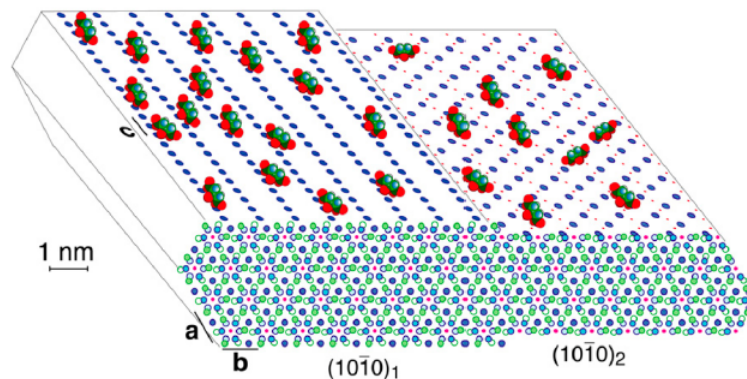
Gomez-Morales et al., *Prog Cryst Growth Charact Mater*, 2013

# Bone apatite

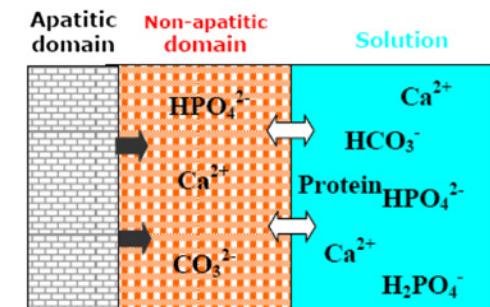
## Chemical-physical features

- Non-stoichiometry. Ca-deficient crystals ( $\text{Ca/P} < 1.67$ )
- Poorly crystalline. Plate shaped crystals 30-50 nm
- Presence of foreign ions (0.9 wt% Na, 0.5 wt% Mg, 3-5 wt%  $\text{CO}_3$ )
- Apatite surface is studded with strongly bound citrate molecules

Analytical method	Crystal dimensions
TEM	20 nm long $\times$ 3-6 nm wide
XRD	10-35 nm long
$\mu$ XRD	(14-17) nm $\times$ (3-5) nm
SAXS	50 nm $\times$ 25 nm $\times$ 1.5-4 nm
SAXS and TEM	30 nm $\times$ 20 nm $\times$ 1.5-2 nm
AFM	(200-30) nm $\times$ (200-30) nm $\times$ (3-10) nm



**a)** Apatite nanocrystal (3D view)



**b)** Apatite nanocrystal in solution (profile)

Hu et al., *PNAS*, 2010

Gomez-Morales et al., *Prog Cryst Growth Charact Mater*, 2013

# Batch Crystallization method

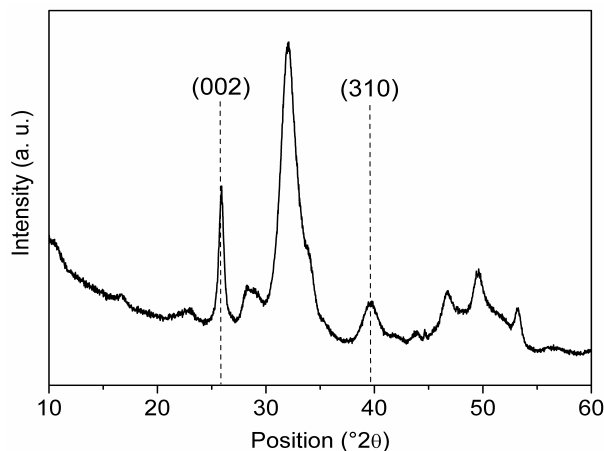
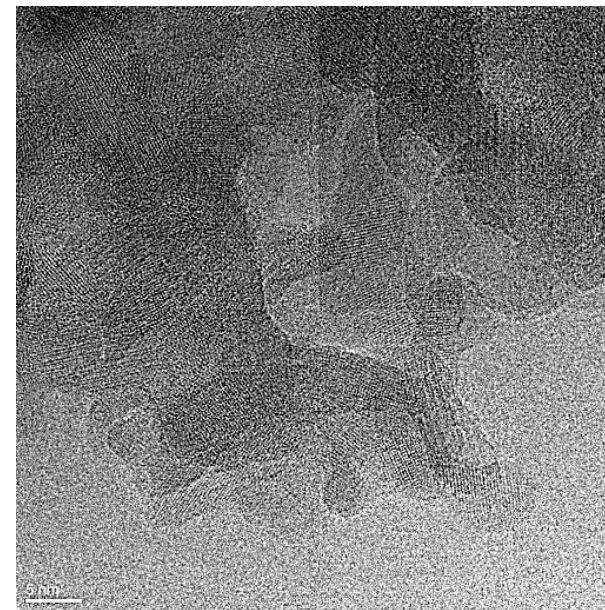
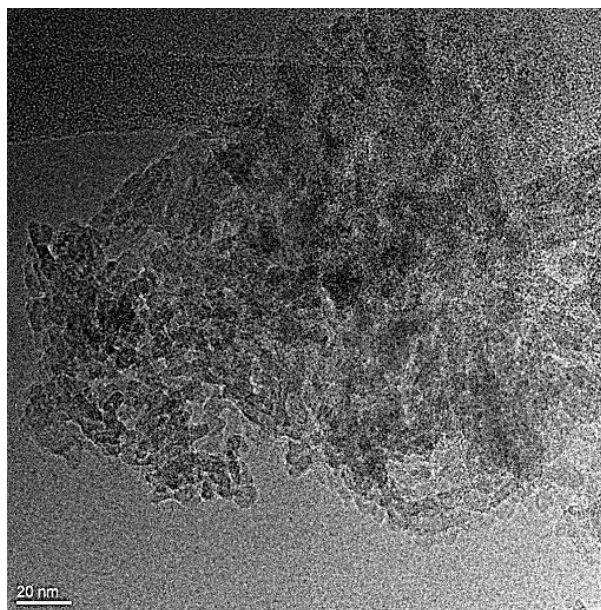


$\text{H}_3\text{PO}_4$

$\text{Ca}(\text{CH}_3\text{COO})_2$

Keeping the pH at 10  
with  $(\text{NH}_4)\text{OH}$ .

Stirring for 24h at room  
temperature.



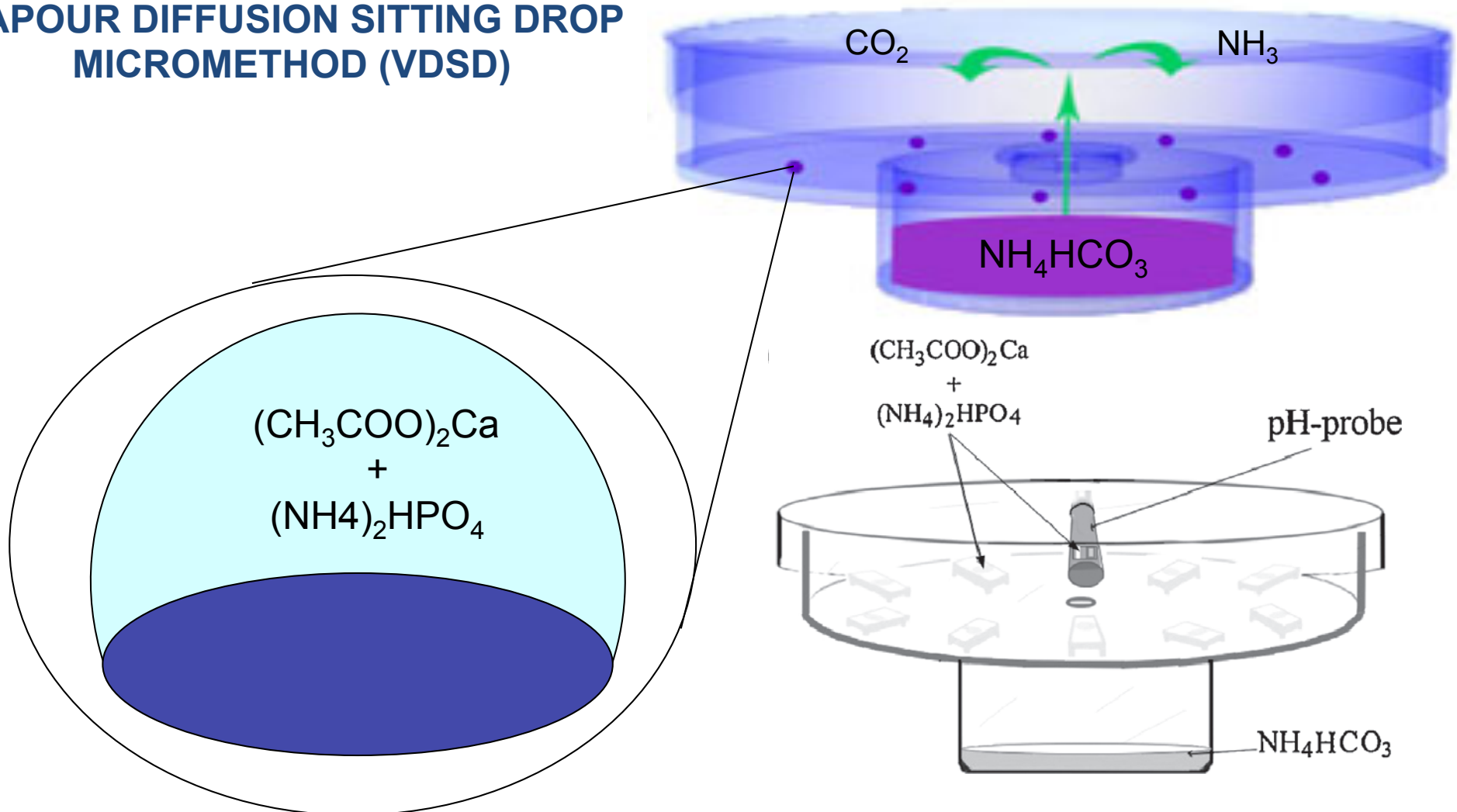
Ca/P (mol) <sup>[a]</sup>	Carbonate Species (wt %) <sup>[b]</sup>	SSA <sub>BET</sub> (m <sup>2</sup> g <sup>-1</sup> )	D <sub>002</sub> (nm) <sup>[c]</sup>	D <sub>310</sub> (nm) <sup>[c]</sup>	Length Dimension s (nm) <sup>[d]</sup>	Degree of crystallinity
1.65	2	160 ± 16	30 ± 5	10 ± 2	20 ± 5	61% ± 5

lafisco et al., *Nanoscale*, 2012  
lafisco et al., *Coll Surf B*, 2010  
lafisco et al., *Dalton Trans*, 2011  
lafisco et al., *Small*, 2013

<sup>[a]</sup>Calculated by ICP-OES. <sup>[b]</sup>Calculated by TGA. <sup>[c]</sup>Calculated applying the Scherrer equation.  
<sup>[d]</sup>Calculated by TEM

# Vapour diffusion Crystallization method

## VAPOUR DIFFUSION SITTING DROP MICROMETHOD (VDSD)



Iafisco et al., *Adv Eng Mat*, 2009; Iafisco et al., *Cryst Res Techn*, 2011; Gomez-Morales et al., *Cryst. Growth Des*, 2011

# Vapour diffusion Crystallization method

## VAPOUR DIFFUSION SITTING DROP MICROMETHOD (VDSD)

- Control of the gas diffusion rate ( $\text{NH}_3$  and  $\text{CO}_2$ ) by simply changing the concentration of  $\text{NH}_4\text{HCO}_3$
- Confinement of the nucleation in microdroplets that closely resemble the in vivo microenvironments where biominerals are deposited.
- Control the rate of pH increase until it reaches an asymptotic value and therefore the rate of droplets supersaturation
- Perform several experiments per run, since as many as 12 drops per mushroom can be used.

Iafisco et al., *Adv Eng Mat*, 2009; Iafisco et al., *Cryst Res Techn*, 2011; Gomez-Morales et al., *Cryst Growth Des*, 2011



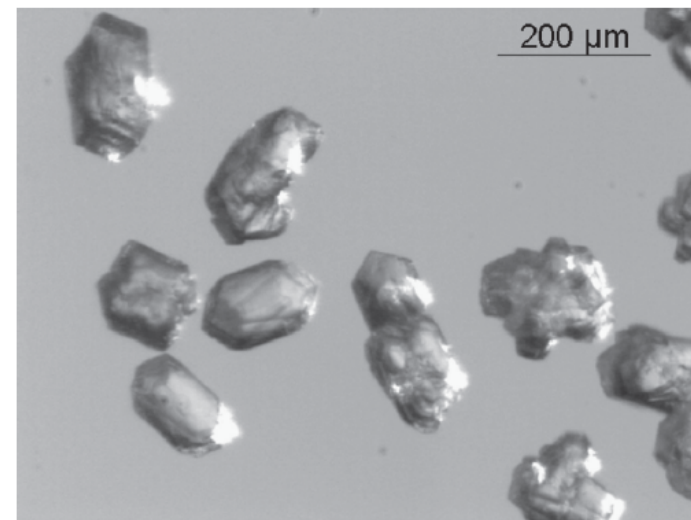
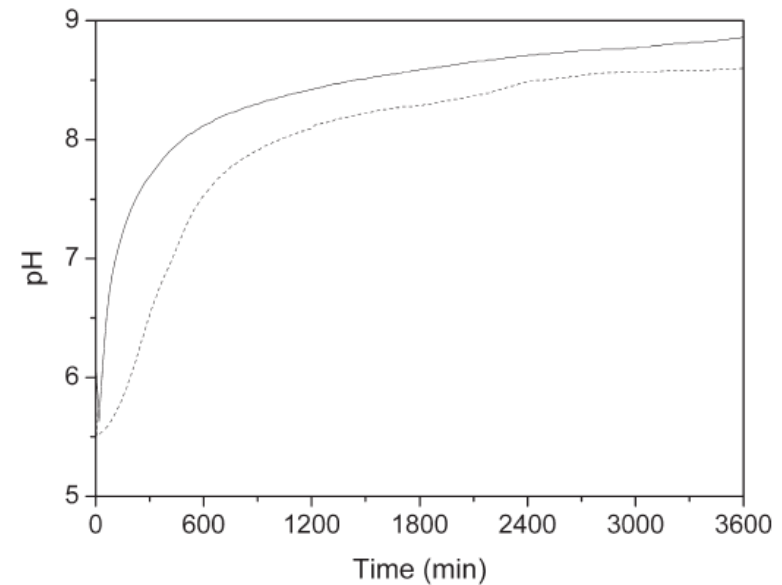
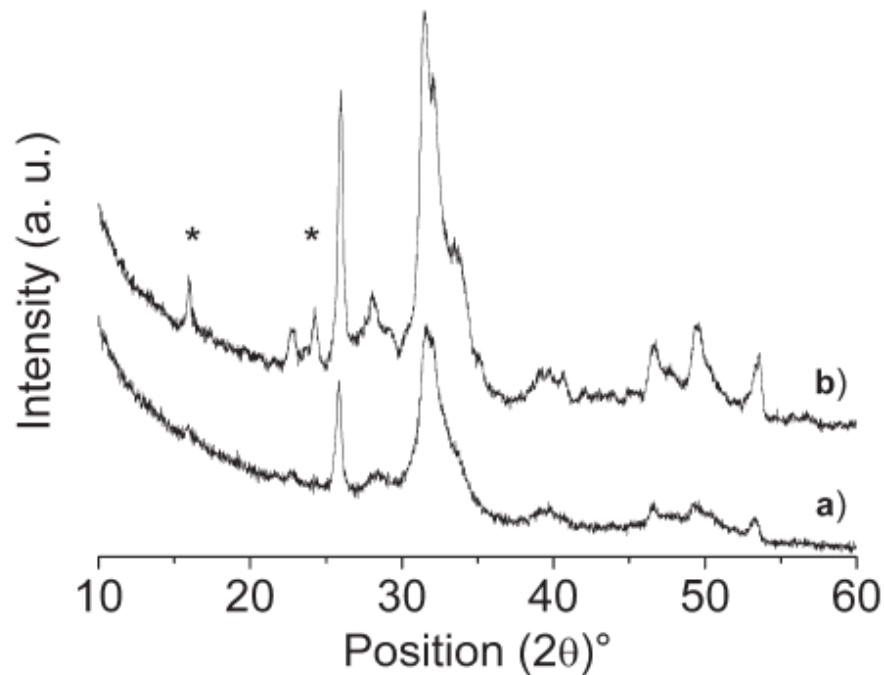
# Vapour diffusion Crystallization method

$\text{Ca}(\text{CH}_3\text{COO})_2$  50mM

$(\text{NH}_4)_2\text{HPO}_4$  30 mM

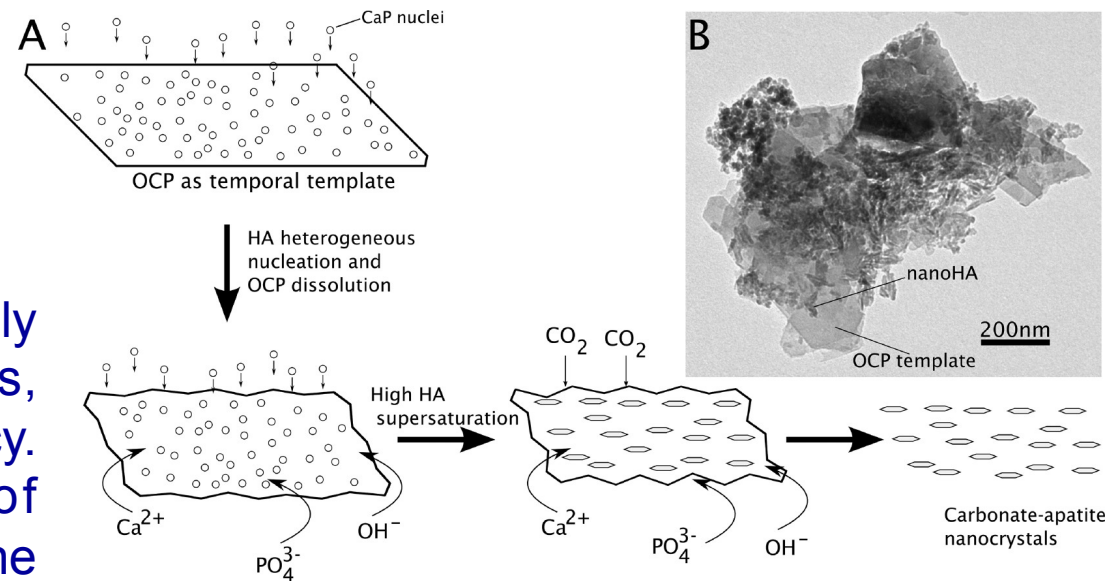
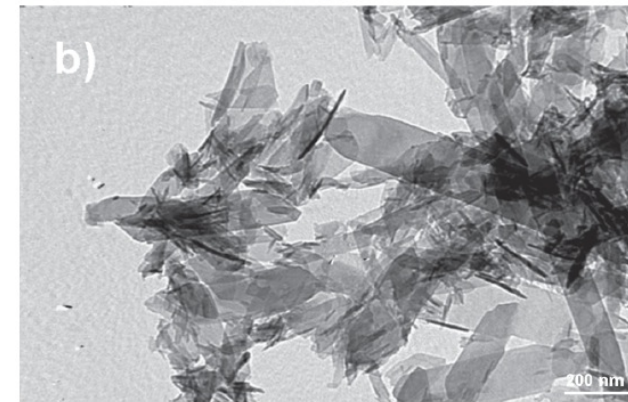
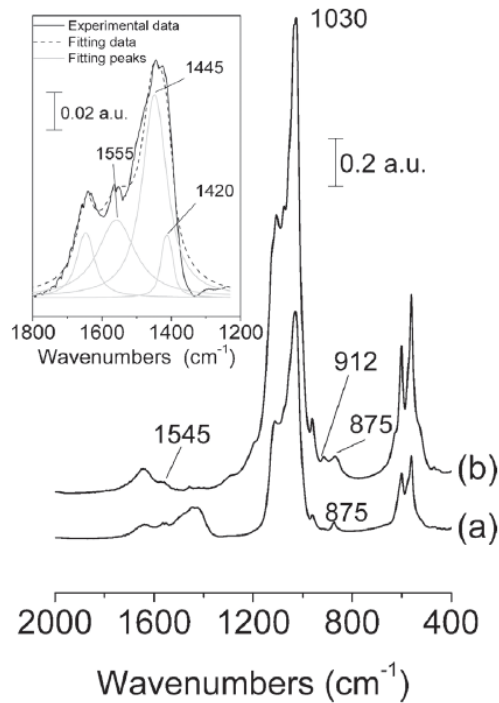
3 mL  $\text{NH}_4\text{HCO}_3$  40mM or 2.1M

Crystallization time 1 day or 1 week



Iafisco et al., *Adv Eng Mat*, 2009; Iafisco et al., *Cryst Res Techn*, 2011

# Vapour diffusion Crystallization method

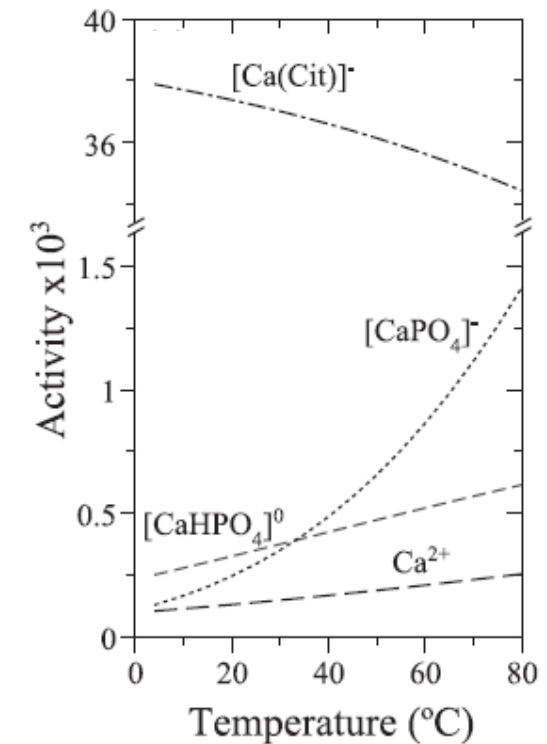
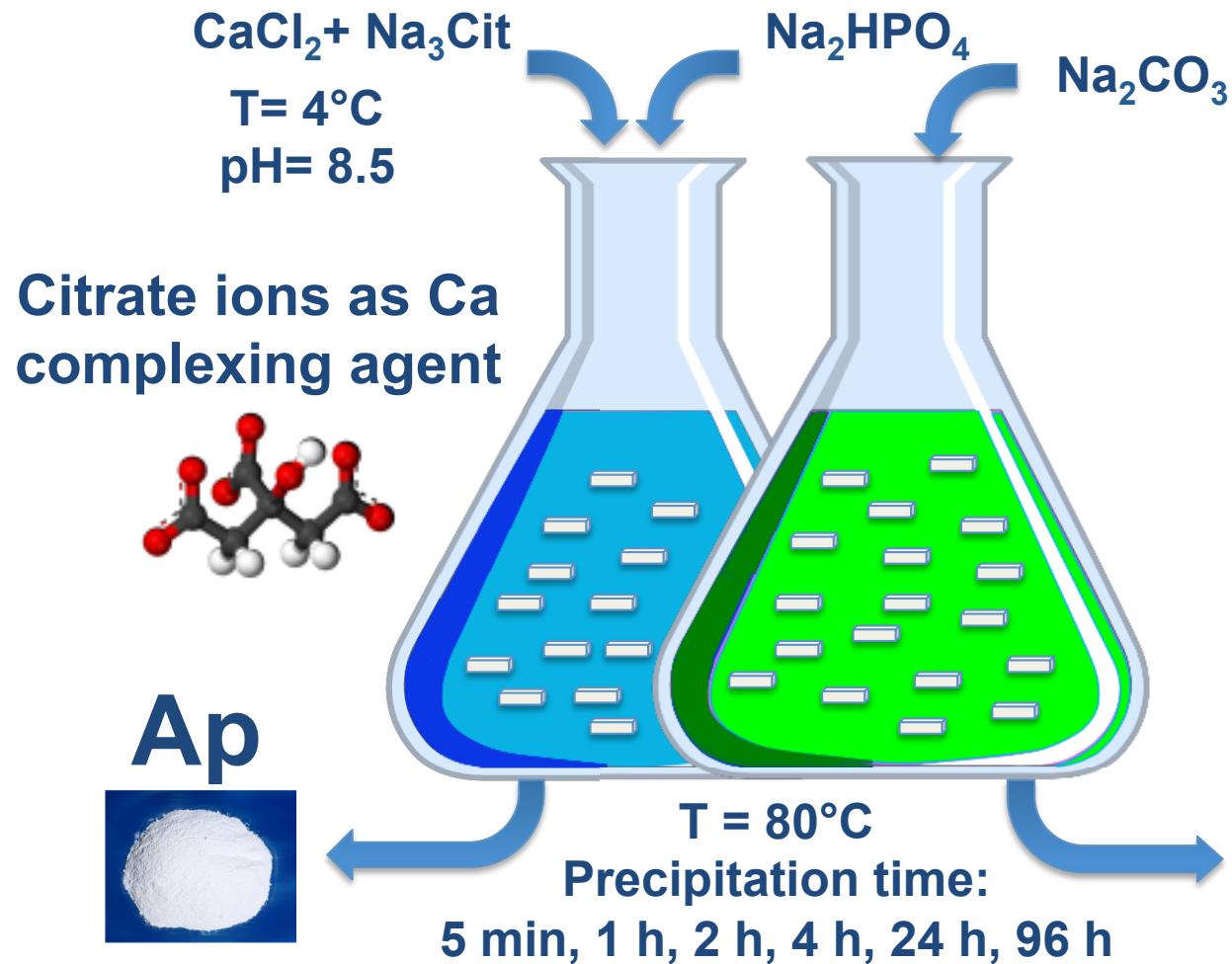


Template stabilizes the heterogeneously nucleated crystals with nano-sizes, minimizing their aggregation tendency. The result is the production of nanocrystals, at the same time that the template dissolves

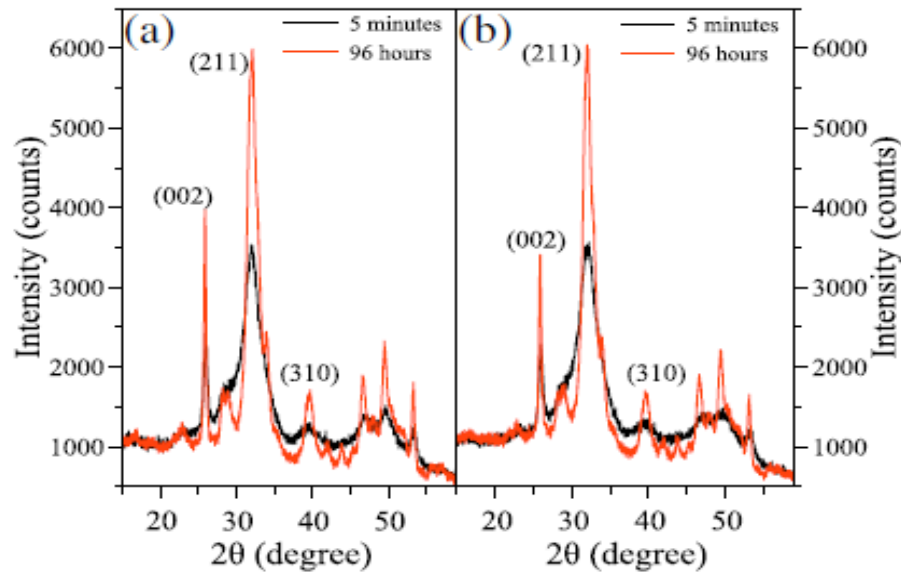
Iafisco et al., *Adv Eng Mat*, 2009; Iafisco et al., *Cryst Res Techn*, 2011

# Thermal decomplexing method

## Thermal decomplexing of metastable Ca / Cit / PO<sub>4</sub> solutions



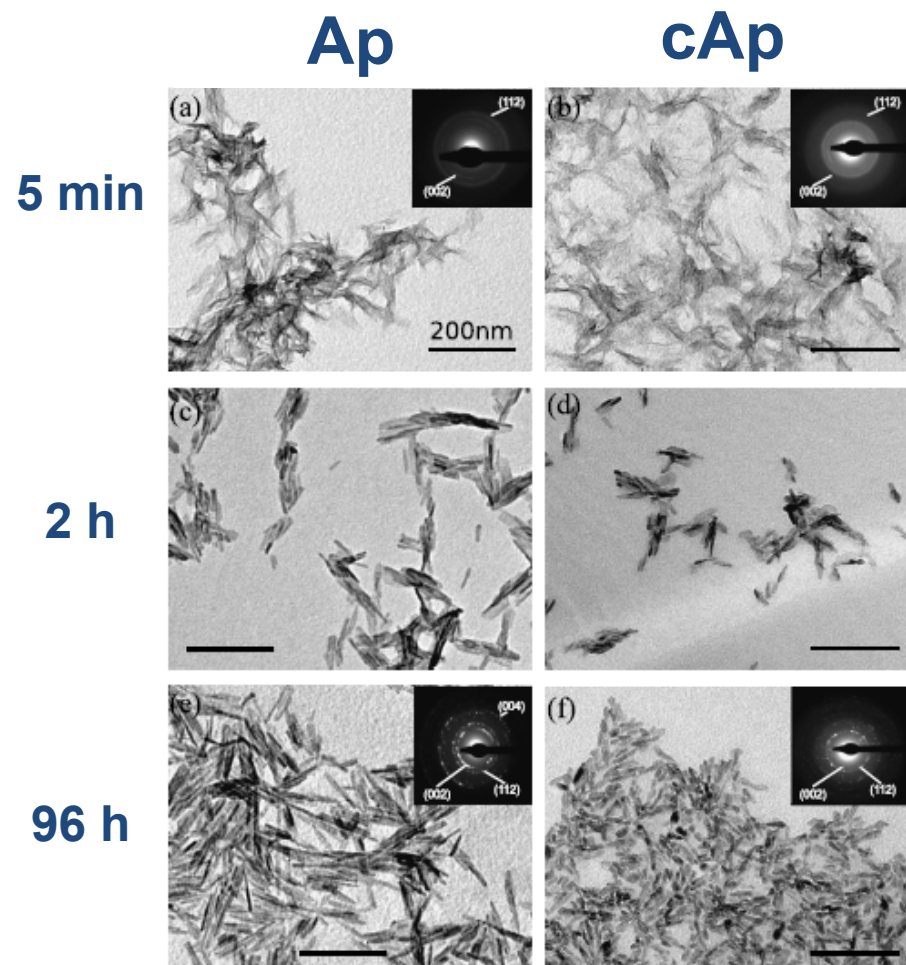
# Thermal decomplexing method



- Pure apatitic phase. Broad peaks close to the biogenic one.
- Crystallinity increases with maturation time
- Citrate and structural water decrease with the maturation time

Precipitation time	Structural water <sup>a</sup> (%wt.)	Citrate <sup>a</sup> (%wt.)	Carbonate <sup>a</sup> (%wt.)	Ca/P <sup>b</sup>
Ap 5 min	5.8 ± 0.2	5.0 ± 0.2	1.5 ± 0.2	1.53
Ap 4 h	3.9 ± 0.1	2.4 ± 0.1	1.1 ± 0.1	1.51
Ap 24h	3.3 ± 0.1	1.9 ± 0.1	1.0 ± 0.1	1.52
Ap 48 h	2.9 ± 0.2	2.1 ± 0.2	1.3 ± 0.2	1.53
Ap 96 h	2.6 ± 0.2	2.0 ± 0.1	1.0 ± 0.1	1.54
cAp 5 min	6.3 ± 0.3	5.9 ± 0.2	1.5 ± 0.1	1.60
cAp 4 h	3.8 ± 0.3	3.3 ± 0.2	1.5 ± 0.1	1.60
cAp 24h	3.6 ± 0.2	3.5 ± 0.2	3.1 ± 0.2	1.59
cAp 48 h	2.6 ± 0.2	2.1 ± 0.1	2.6 ± 0.3	1.59
cAp 96 h	2.5 ± 0.1	2.1 ± 0.1	2.9 ± 0.2	1.58

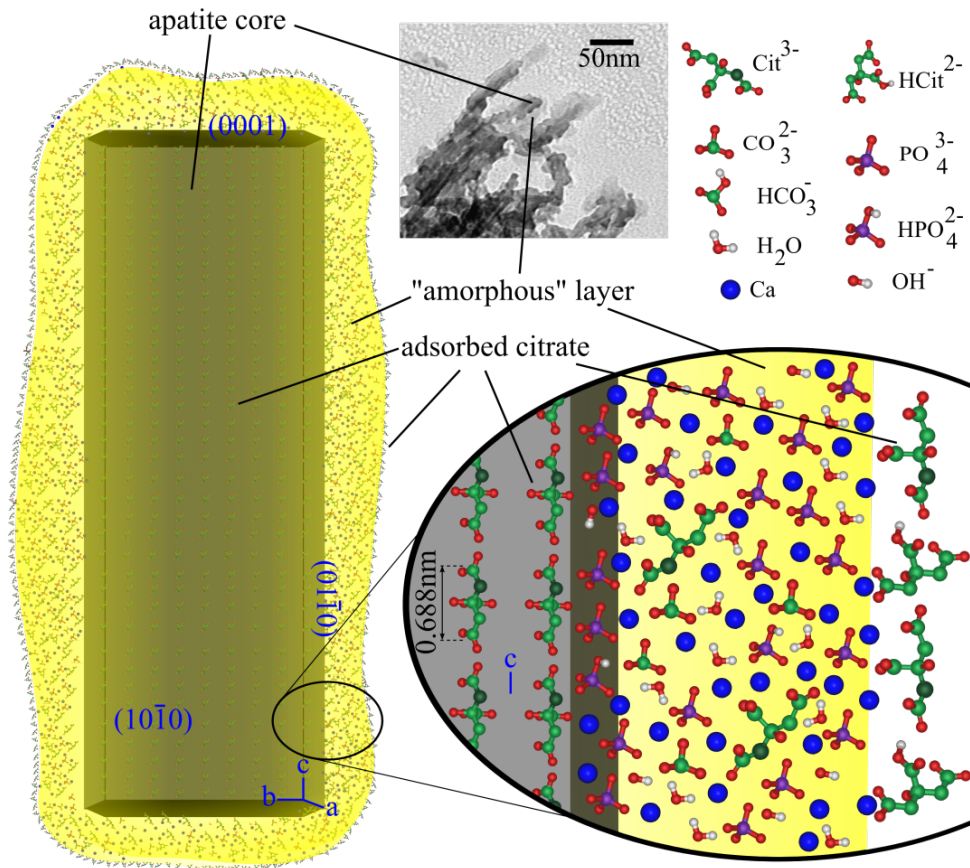
# Thermal decomplexing method



The precipitation time and the carbonate strongly affect the chemical composition, the dimensions and the crystallinity

Precipitation time	L [nm]	W [nm]	R	D <sub>002</sub> [nm]	D <sub>310</sub> [nm]
Ap 5 min	99 ± 30	21 ± 5	4.7 ± 1.2	19.4	4.0
Ap 1 h	45 ± 24	12 ± 7	4.0 ± 1.3	37.1	5.9
Ap 2 h	75 ± 27	15 ± 6	5.5 ± 2.4	48.0	6.3
Ap 4 h	85 ± 16	16 ± 4	5.6 ± 1.3	45.3	6.5
Ap 24 h	84 ± 32	14 ± 6	6.9 ± 3.0	48.0	8.6
Ap 96 h	104 ± 43	15 ± 6	7.6 ± 3.2	90.6	9.6
cAp 5 min	109 ± 16	27 ± 5	4.3 ± 1.3	17.0	5.2
cAp 1 h	49 ± 18	10 ± 5	5.4 ± 1.9	22.6	5.9
cAp 2 h	60 ± 24	17 ± 6	3.7 ± 1.3	30.2	5.6
cAp 4 h	55 ± 10	18 ± 3	3.2 ± 0.9	35.4	6.1
cAp 24 h	40 ± 15	12 ± 3	3.7 ± 1.5	31.3	5.7
cAp 96 h	29 ± 10	12 ± 3	2.5 ± 1.0	45.3	8.0

# Thermal decomplexing method



- Composed of a well-ordered carbonate-substituted apatitic core embedded in a non-apatitic hydrated layer containing citrate ions
- This layer transforms into a more stable apatite domain upon maturation in aqueous media
- Excellent biocompatibility since they were not cytotoxic to a mouse carcinoma cell line up to a final concentration of  $100 \mu\text{g ml}^{-1}$

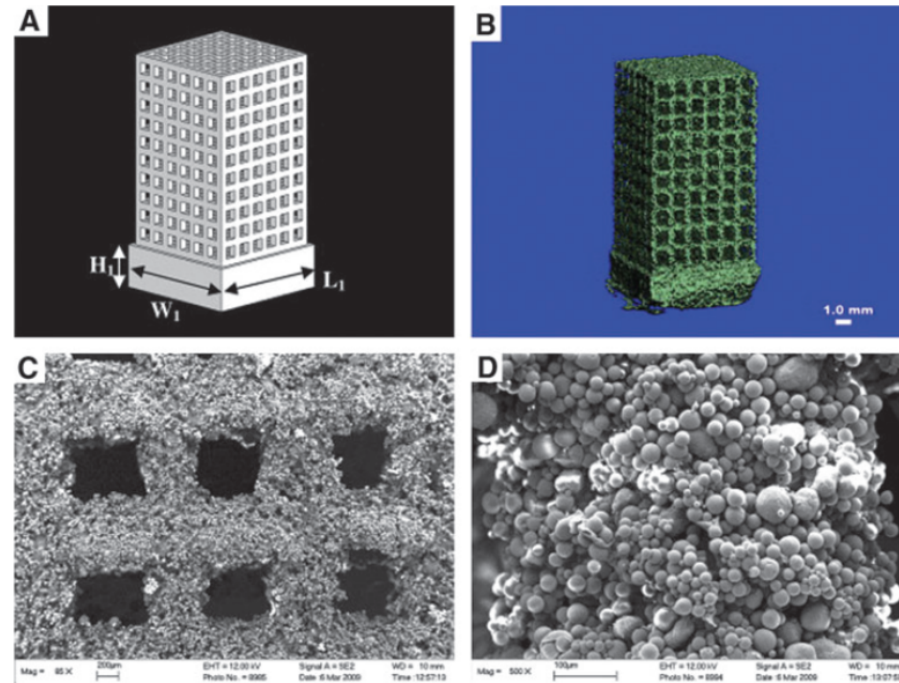
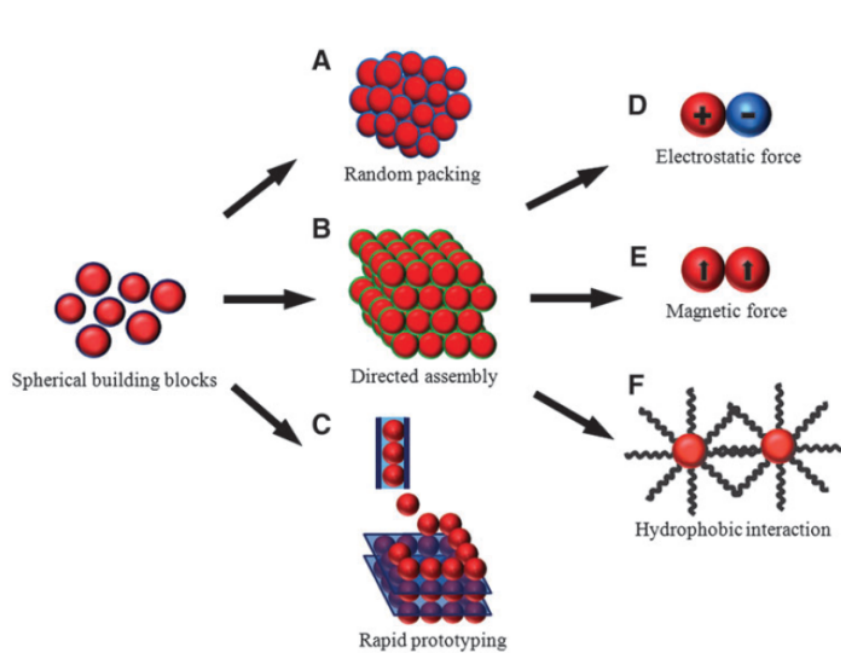
# Organic-Inorganic Composites

- The main goal of bone tissue engineering is the development of biocompatible and biodegradable materials and the preparation of porous scaffolds with adequate mechanical properties for filling large bone defects
- The major limitations to use apatites as load bearing biomaterials are their mechanical properties, namely, they are brittle with a poor fatigue resistance.
- Natural bone structure, is composed of organic and inorganic materials, thus it is rational to use both of them to form composite scaffolds, giving advantages over each single component in terms of physical and biological properties
- Polymer–apatite composites can combine a better structural integrity and flexibility along with good bioactivity, biocompatibility and biodegradability

# Micro-nano-spheres

## Micro-nano-spheres based scaffolds

- Dispersed phase surrounded by a continuous matrix (solid polymers, hydrogel polymers, CaP cements)
- Building blocks to establish integral scaffolds without surrounding matrix by a bottom up approach or rapid prototyping.

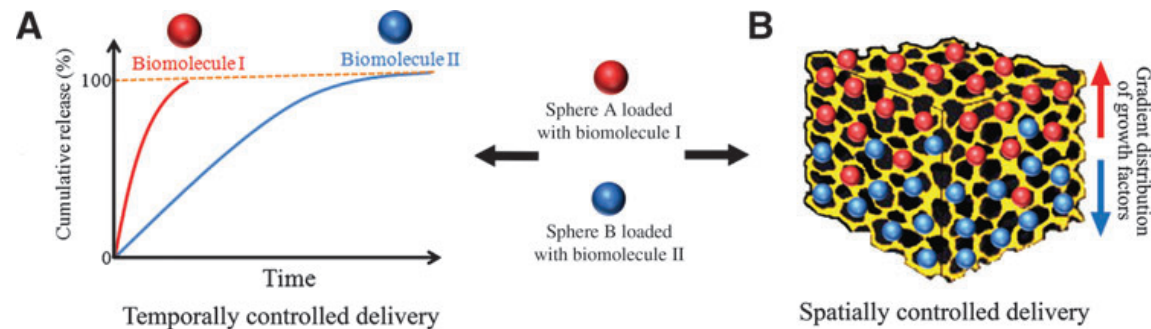


Wang et al. *Tissue Eng B*, 2012  
Duan et al. *Acta Biomater*, 2010

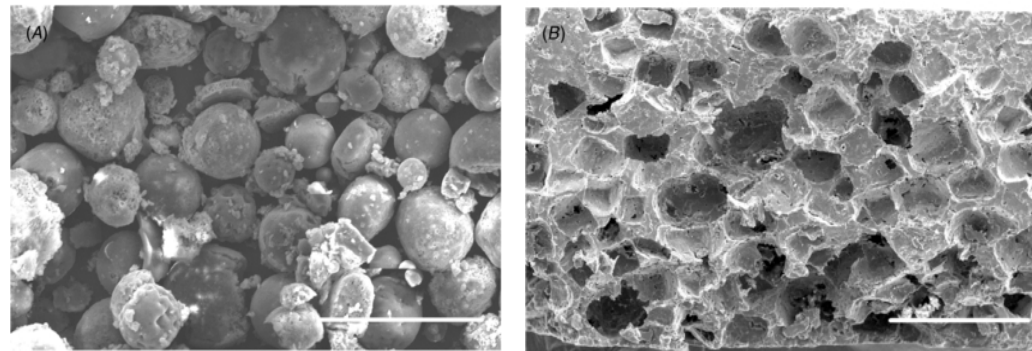
# Micro-nano-spheres

Micro-nano-spheres based scaffolds can display several advantages:

- Improving control over sustained delivery of therapeutic agents, signalling biomolecules and even pluripotent stem cells



- Introducing porosity and/or improve the mechanical properties of bulk scaffolds by acting as porogen or reinforcement phase



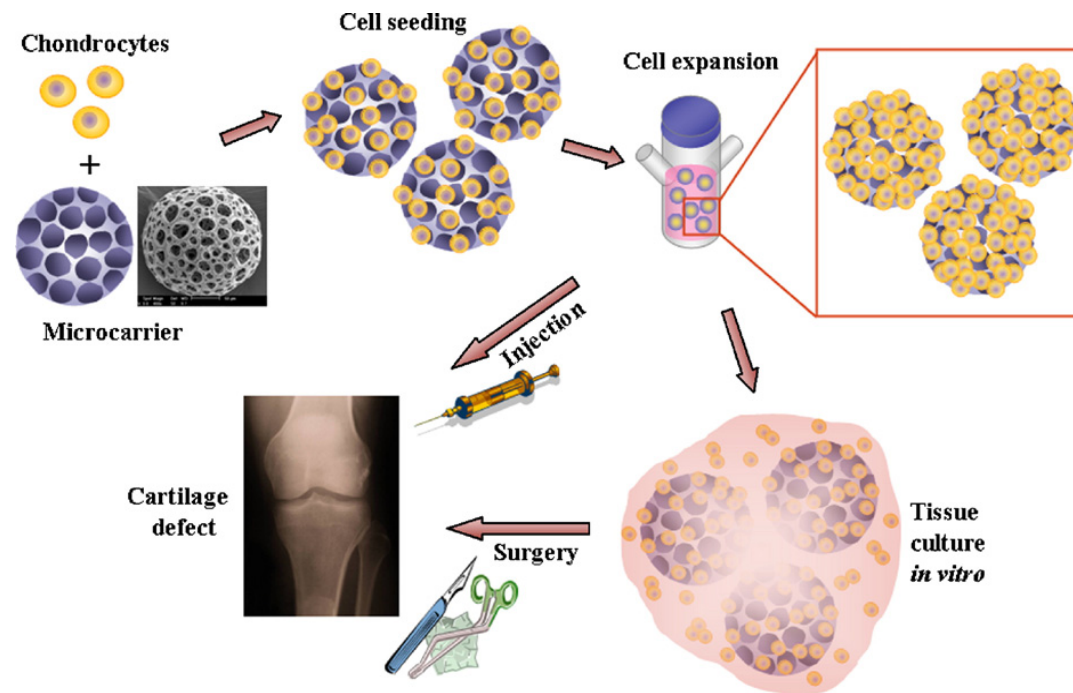
Wang et al., *Tissue Eng B*, 2012

Ravi et al., *Biomed Mater*, 2012

# Micro-nano-spheres

Micro-nano-spheres based scaffolds can display several advantages:

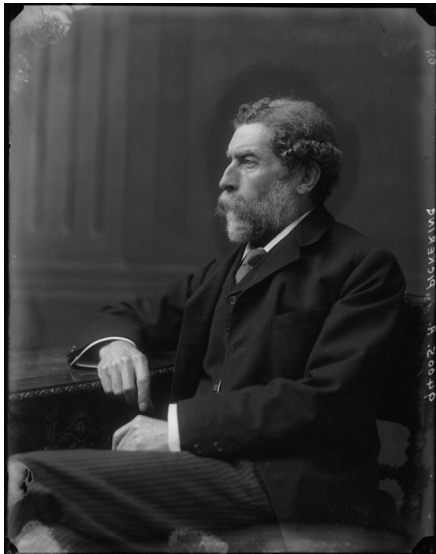
- Supplying compartmentalized micro-reactors for dedicated biochemical processes, functioning as cell delivery vehicle
- Giving possibility of preparing injectable and/or mouldable formulations to be applied by using minimally invasive surgery



Chung and Park, *Adv Drug Delivery Rev*, 2007

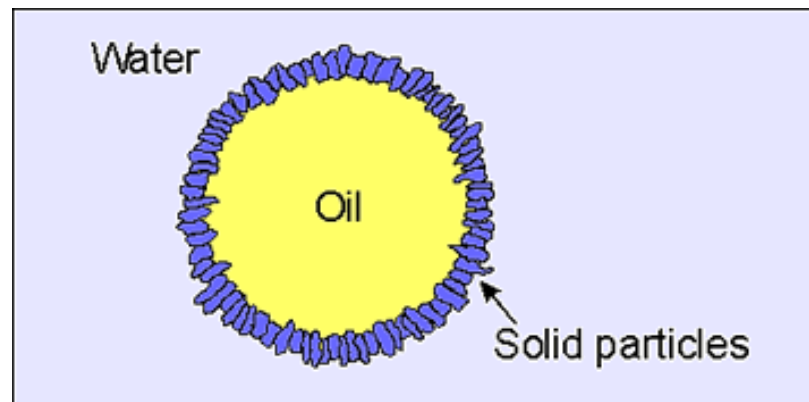
# Pickering emulsion

Pickering emulsions are solid particle-stabilized emulsions in the absence of any molecular surfactant, where solid particles adsorbed to an oil–water interface.



© National Portrait Gallery, London

## Percival Spencer Umfreville Pickering (1858-1920)



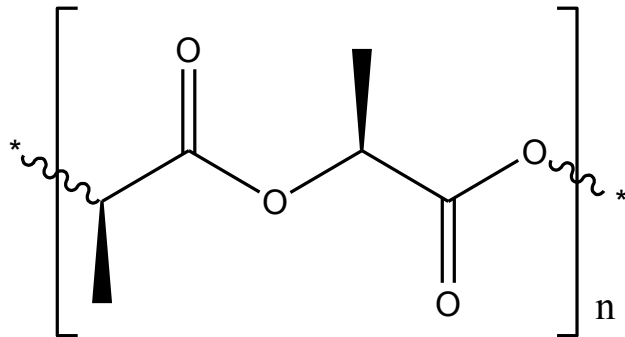
- Contact Angle
- Particle Size
- Solid Concentration
- Interparticulate interaction

Pickering emulsions require sufficiently small particles which arrange in the o/w interface. The solid particles usually are **at least 10-fold smaller** in size than the dispersed droplets of the emulsion.

A wide range of particles (silica, metals, cellulose, apatite, starch, clays, microgels, and polystyrene) have been recently reported to be effective Pickering emulsifiers.

Pickering S U, *J Chem Soc Trans*, 1907

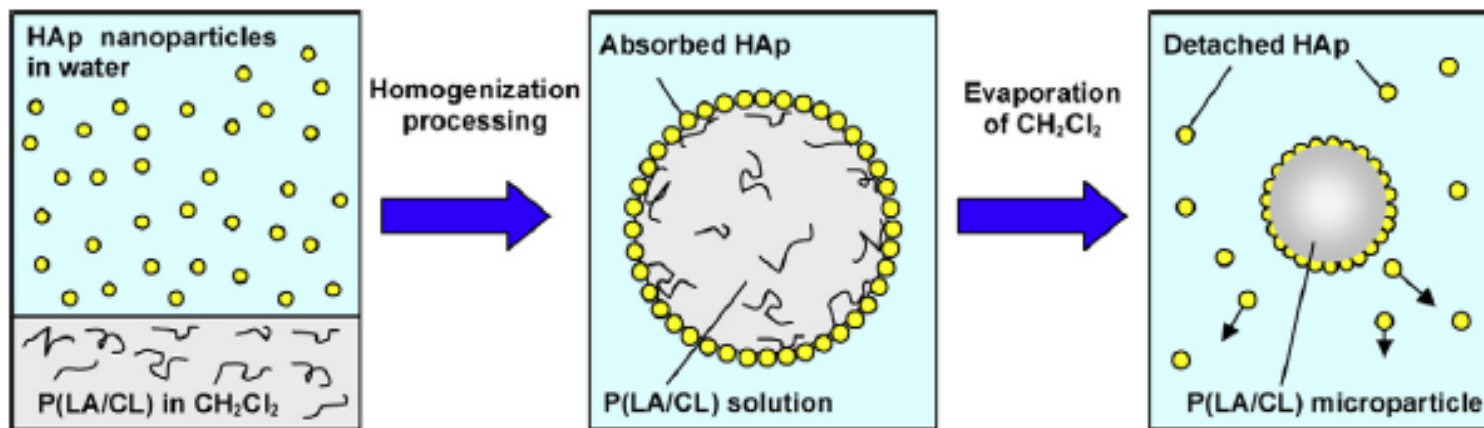
# PLLA-HA microspheres



## Poly(L-lactic) acid (PLLA)

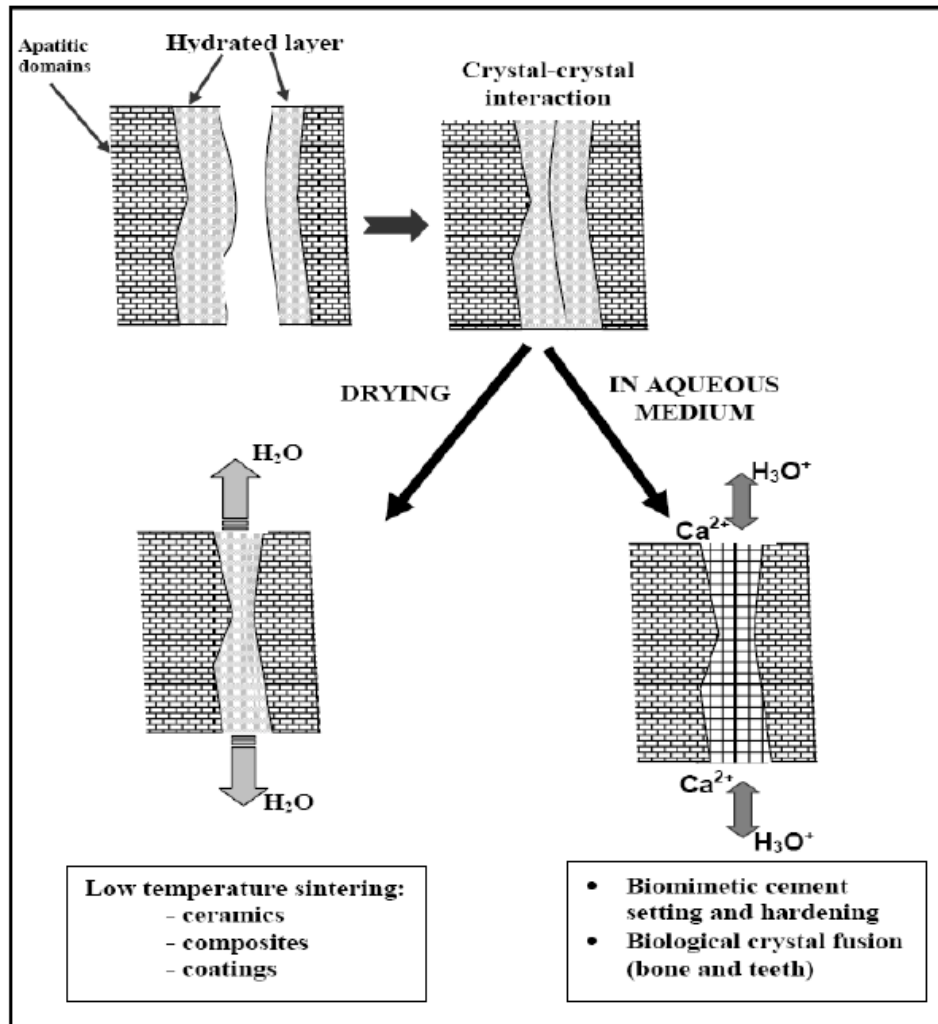
High biocompatibility, hydrolytic degradation, good mechanical properties and ease of manufacture

Aqueous dispersions of HA with solid content of 0.005, 0.01 and 0.02 wt% were prepared and manually shaken for 3 min with the  $\text{CH}_2\text{Cl}_2$  solution of PLLA (1.0 wt% solid content) at room temperature.



Emulsion droplets of  $\text{CH}_2\text{Cl}_2$  solution of PLLA were stabilized by the HA nanocrystals. Subsequent evaporation of  $\text{CH}_2\text{Cl}_2$  leads to the formation of the hollow microspheres.

# PLLA-HA microspheres



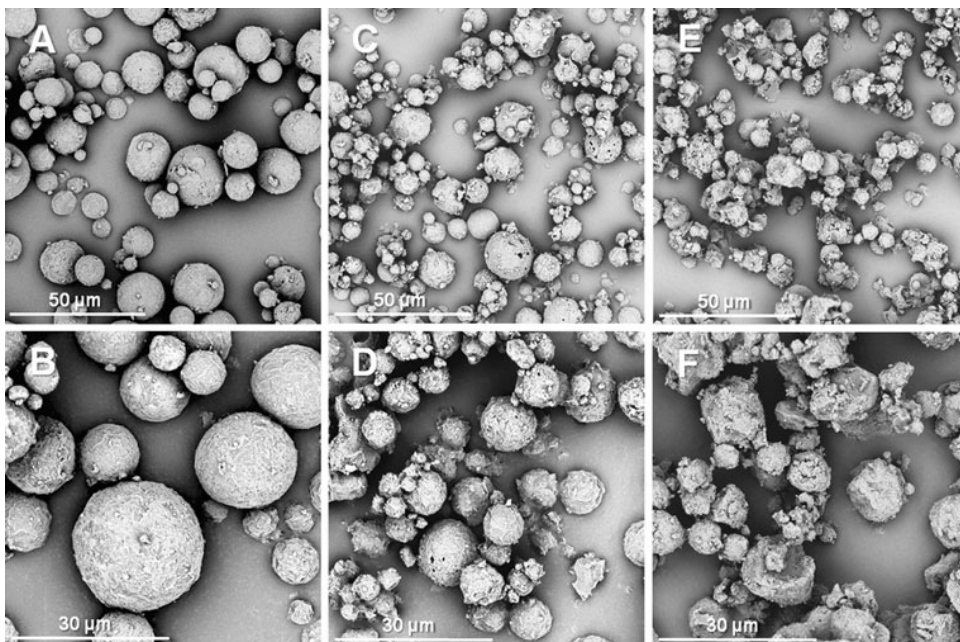
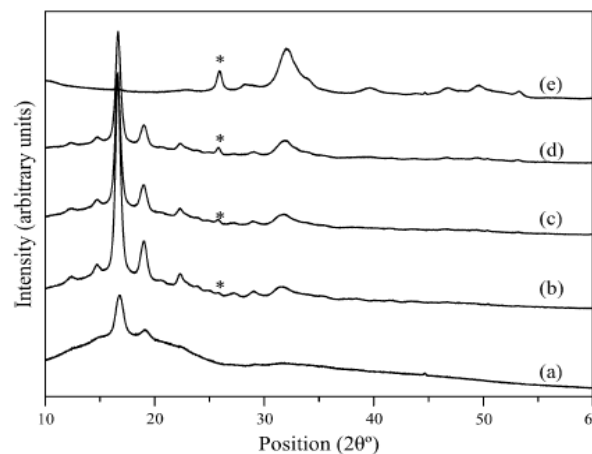
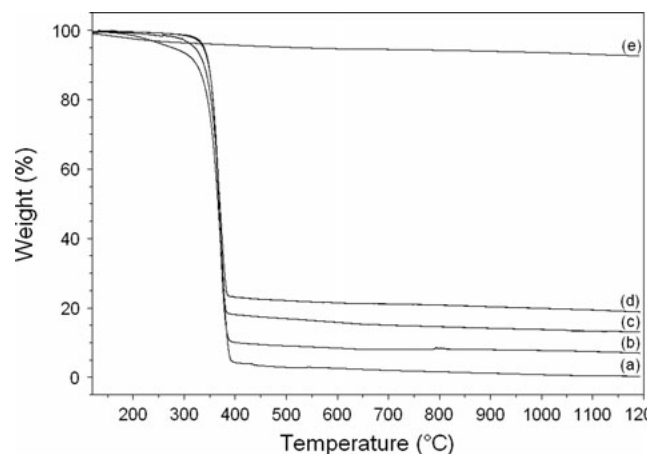
The nanocrystals were not completely dried to avoid their aggregation.

The hydrated layer is involved in cohesiveness and adhesion between two apatite nanocrystals and the progressive drying increases intercrystal or crystal-substrate contacts.

Upon drying, the steady elimination of excess water molecules brings two crystals together, enabling the constitutive ions to interact by means of a strong electrostatic interaction. At the end of the process, crystals that have been joined cannot be split apart by simple rehydration.

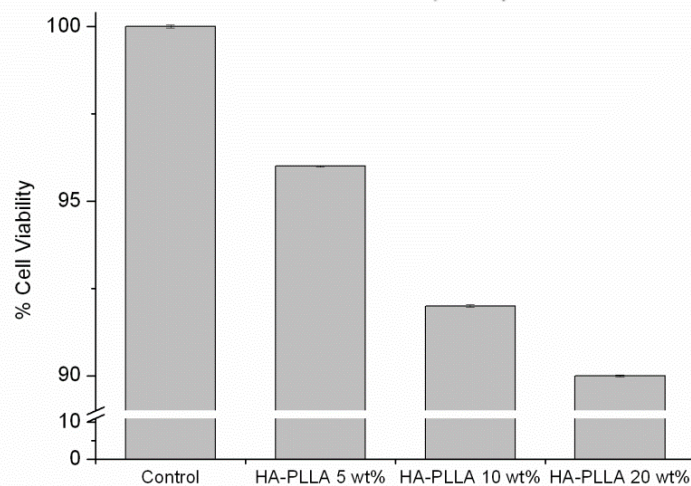
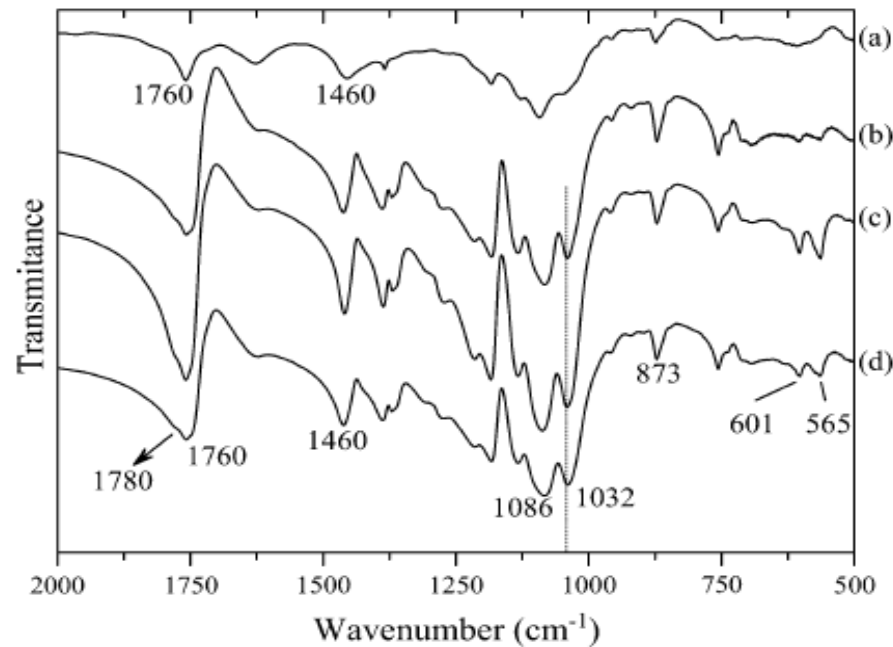
# PLLA-HA microspheres

PLLA hollow microspheres at three different HA surface coverage (5-10-20 wt%), ranging from 10 to 50  $\mu\text{m}$ , were produced. The increase of the HA decreases the size of the spheres, due to the increase of the PLLA surface shrinkage tension.

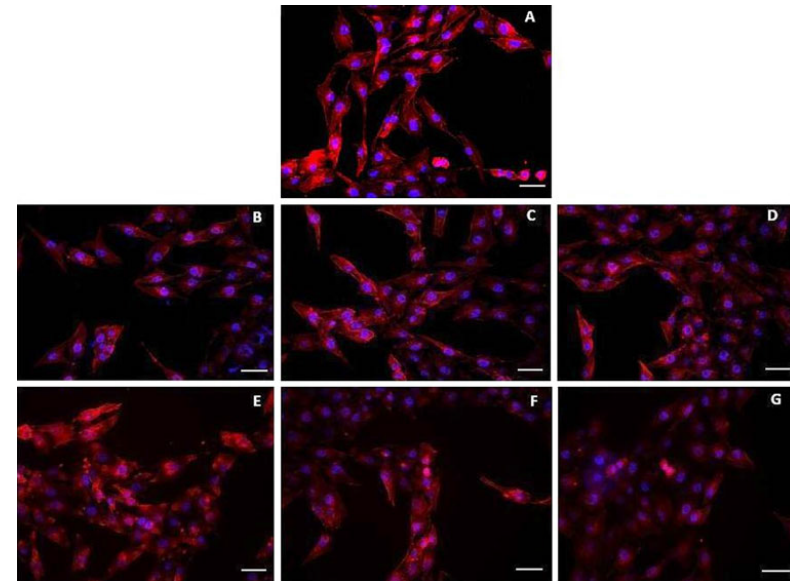


	Particle diameter by microscopy analysis	$\zeta$ -Potential (mV) (pH 6.5)
PLLA	–	$-30.7 \pm 8.1$
Nano HA	20–50 nm [5]	$-7.6 \pm 5.3$
Nano HA–PLLA 5 wt%	5.6 % (>20 $\mu\text{m}$ )	$-30.9 \pm 7.6$
	18.3 % (15–20 $\mu\text{m}$ )	
	25.4 % (15–10 $\mu\text{m}$ )	
	50.7 % (<10 $\mu\text{m}$ )	
Nano HA–PLLA 10 wt%	1.4 % (>20 $\mu\text{m}$ )	$-22.5 \pm 5.3$
	5.6 % (15–20 $\mu\text{m}$ )	
	14.1 % (15–10 $\mu\text{m}$ )	
	78.9 % (<10 $\mu\text{m}$ )	
Nano HA–PLLA 20 wt%	21.1 % (15–20 $\mu\text{m}$ )	$-17.6 \pm 6.0$
	36.6 % (15–10 $\mu\text{m}$ )	
	42.3 % (<10 $\mu\text{m}$ )	

# PLLA-HA microspheres



Interaction of Ca ions of HA with the carbonyl groups of PLLA



High level of cytocompatibility towards fibroblasts (indirect contact) and osteoblasts (indirect and direct contact)

# Magnetic materials

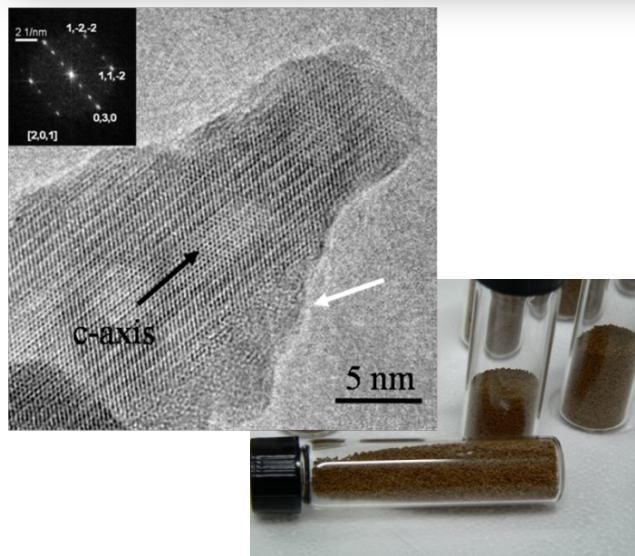
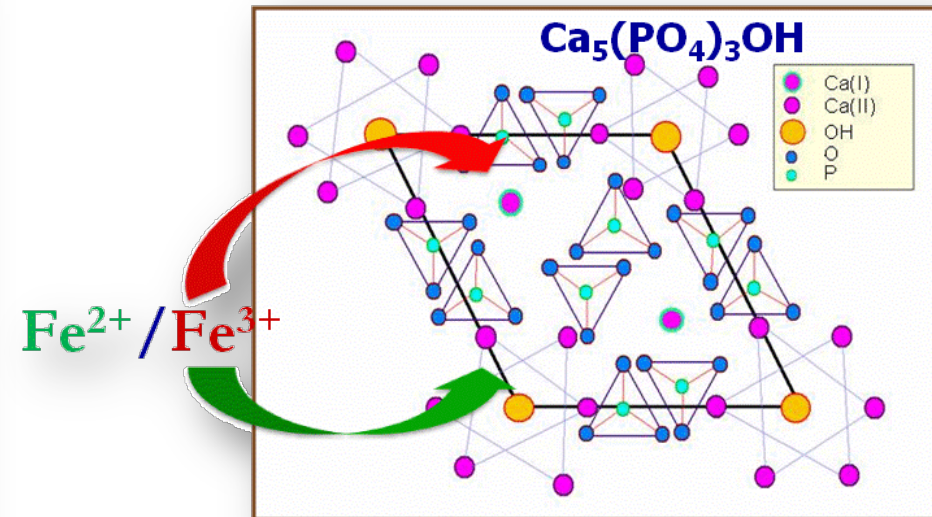
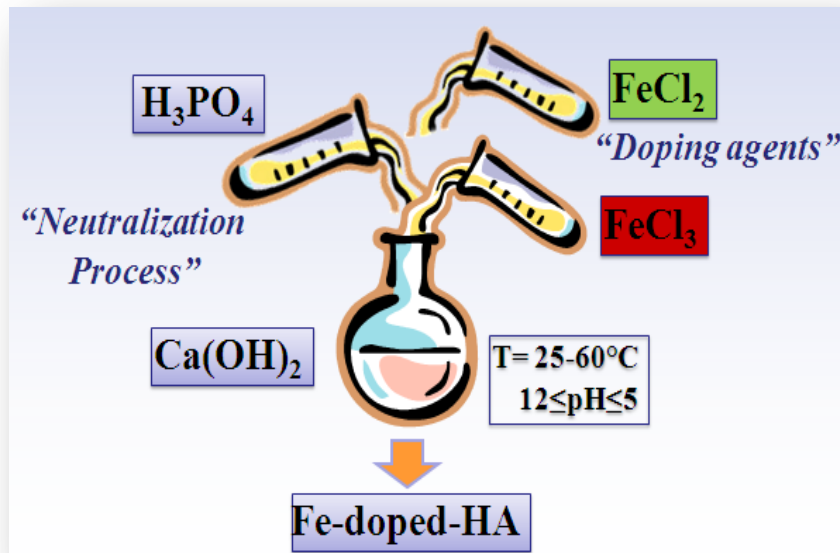
- Magnetic micro-nanoparticles have been progressively employed as support materials for enzyme immobilization, drug-delivery vehicles, contrast agents for magnetic resonance imaging, heat mediators for hyperthermia-based anticancer treatments, and many other exciting biomedical applications.
- Magnetic materials have also recently attracted a big interest in the field of bone tissue regeneration because it has been demonstrated that magnetic nanoparticles have the effect of osteoinduction even without external magnetic force.
- Magnetic scaffolds may provide great potential in bone regenerative medicine, in fact several papers reported that the introduction of magnetic nanoparticles to CaP bioceramics could promote bone formation and cell growth in vitro and in vivo

Sensenig et al., *Nanomedicine*, 2012

Xu et al., *Nano Letters*, 2012

Panseri et al., *Plos One*, 2012

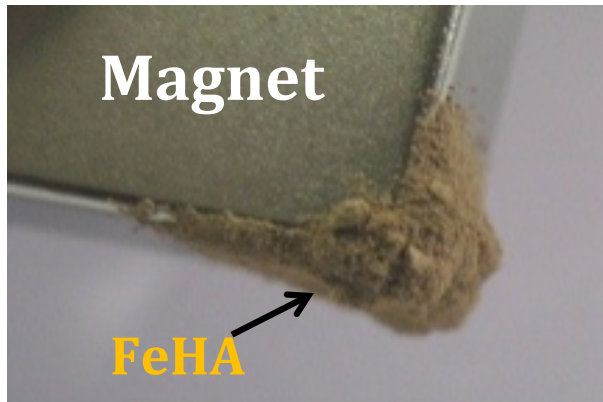
# Magnetic FeHA



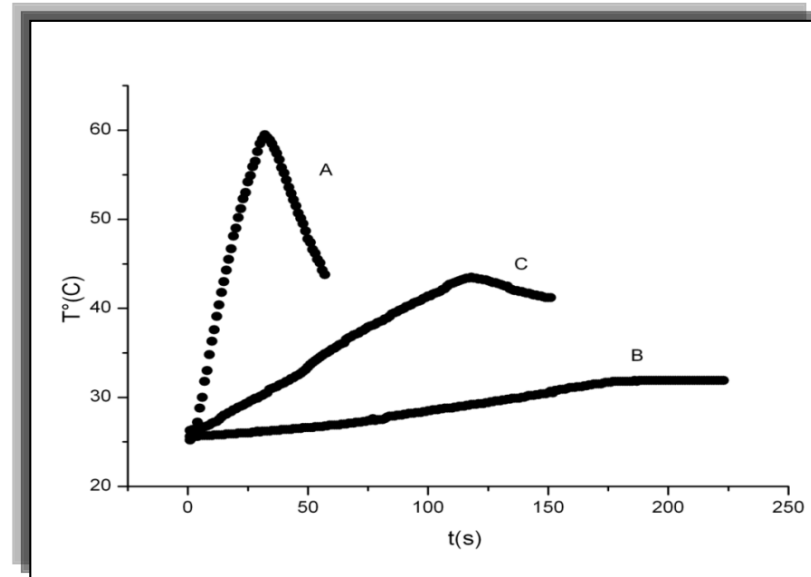
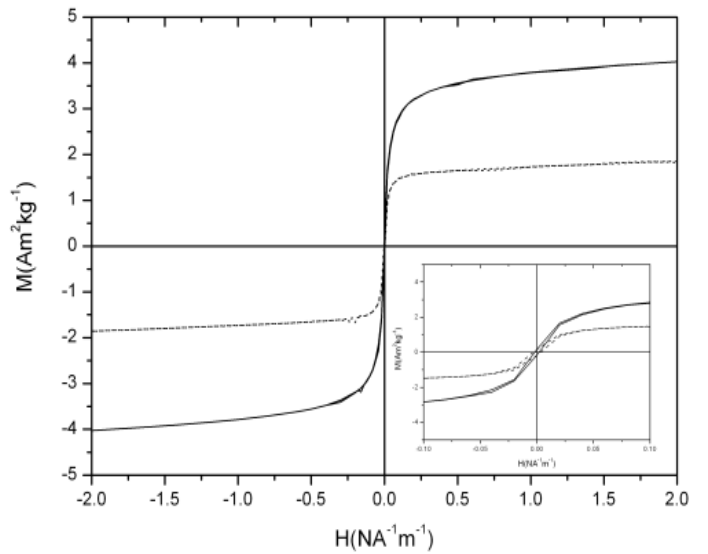
- Introduction of Fe(II) and Fe(III) ions in the correct Ca(1) and Ca(2) sites in order to generate two different sub-lattice able to induce superparamagnetic properties
- Avoid the formation of a magnetite phase
- Dimension: 100 nm in length

Tampieri et al., *Acta Biomater*, 2012

# Magnetic FeHA



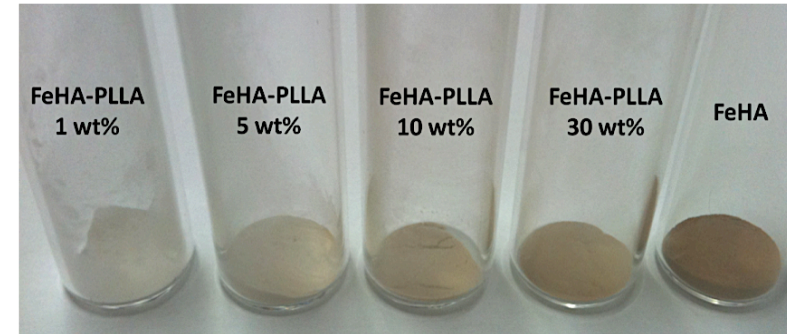
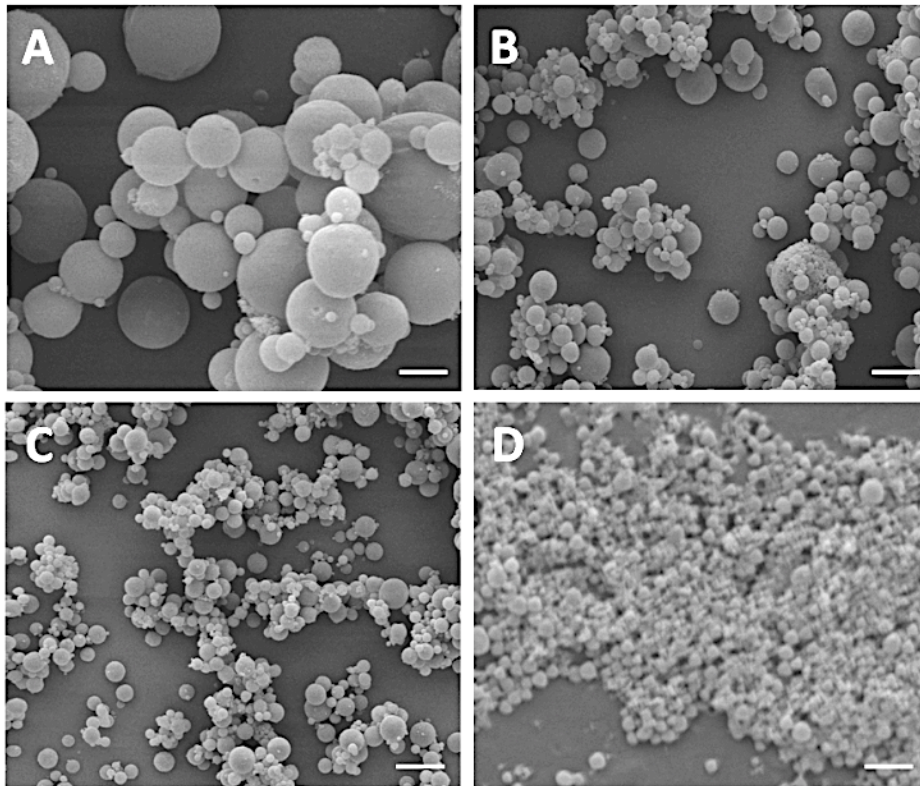
**Superparamagnetic behaviour**  
**Magnetization: 4.0 emu/g**



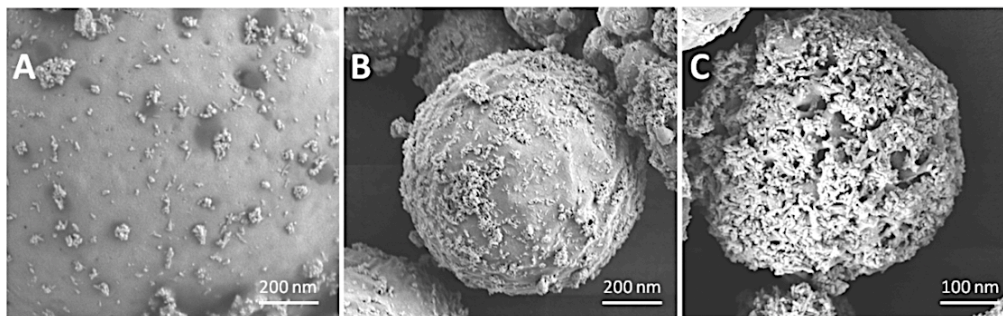
## Hyperthermia evaluation

Magnetic FeHA powder exhibits an increase of temperature of about  $40^{\circ}\text{C}$  in 60s. An higher hyperthermia effect for the magnetic Fe-HA is evident in comparison with the HA-magnetite mixtures

# PLLA-FeHA magnetic micro-nanospheres

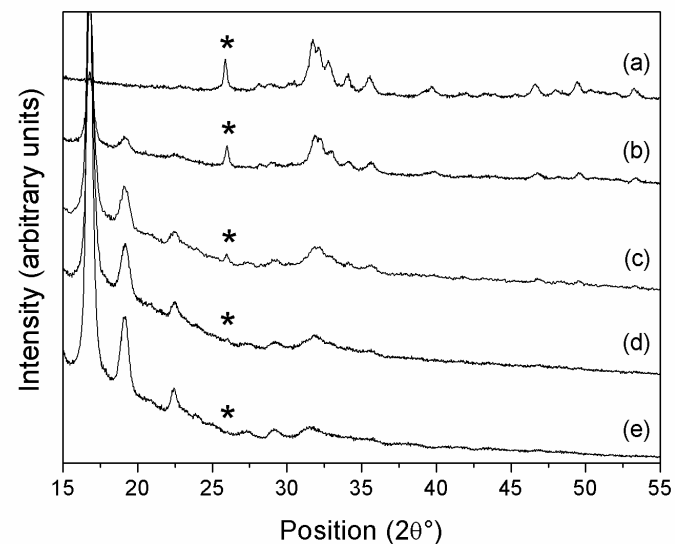
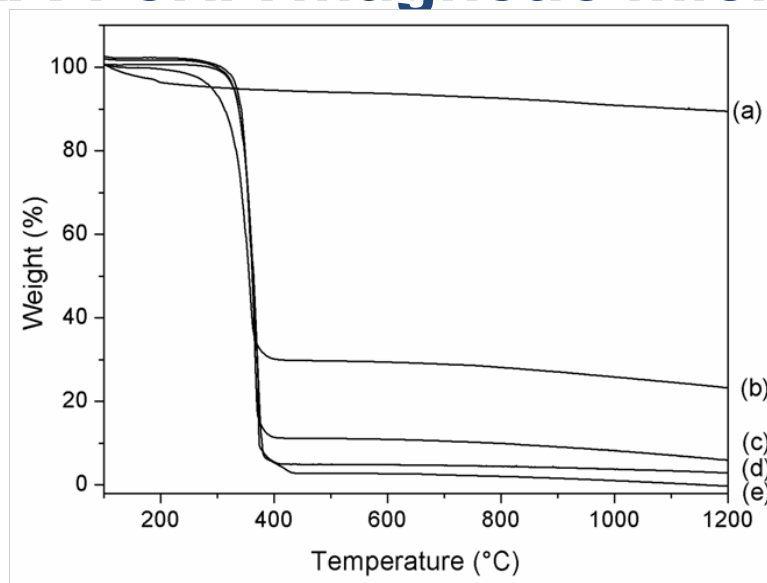


SEM images of FeHA-PLLA composites at different FeHA surface coverage ((A) 1, (B) 5, (C) 10 and (D) 30 wt%). Scale bars are 2 μm.



FEG-SEM images of the surface of (A) FeHA-PLLA 1 wt%, (B) FeHA-PLLA 10 wt% (C) FeHA-PLLA 30 wt%.

# PLLA-FeHA magnetic micro-nanospheres

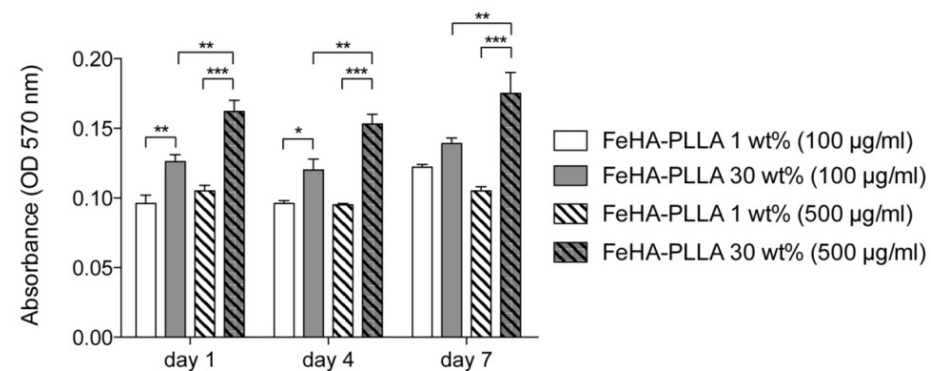
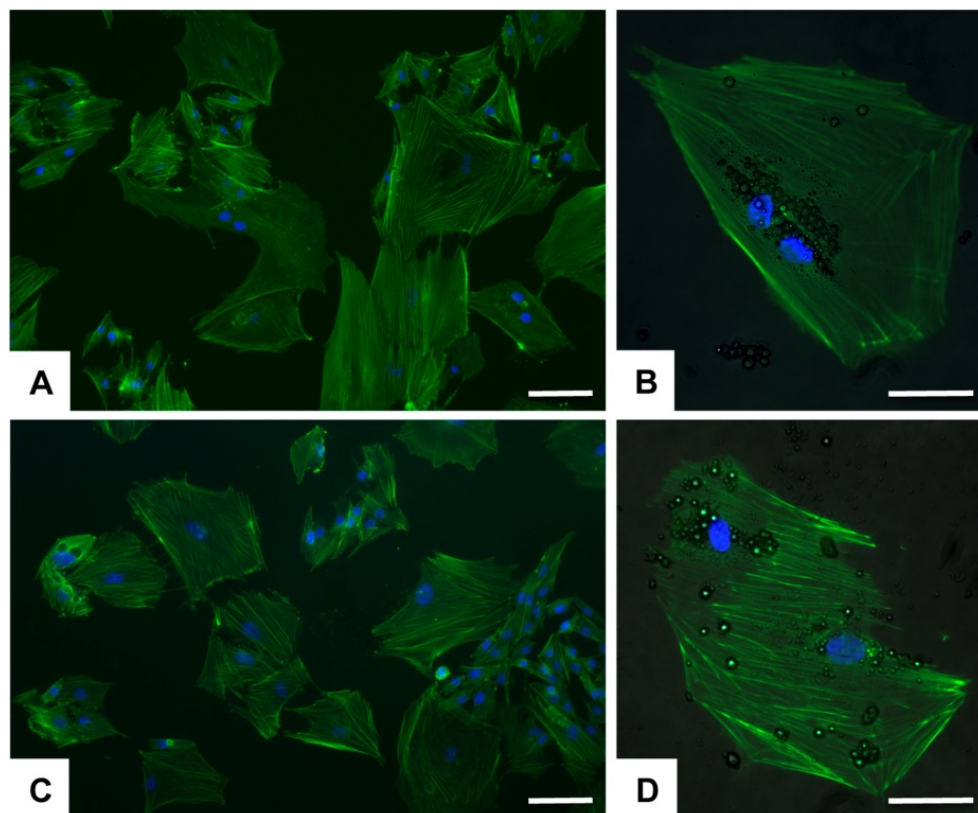


Sample	Size Distribution (nm)	ζ-Potential (mV) (pH 6.5)	Magnetic moment (emu/g)
FeHA	96.0 ± 32.6	-7.9 ± 2.0	0.391 ± 0.011
FeHA-PLLA 1 wt%	1837.0 ± 298.0	-30.7 ± 3.5	-
FeHA-PLLA 5 wt%	633.6 ± 101.6	-23.2 ± 4.2	0.011 ± 0.001
FeHA-PLLA 10 wt%	497.8 ± 63.3	-14.1 ± 3.2	0.035 ± 0.002
FeHA-PLLA 30 wt%	301.9 ± 52.1	-8.9 ± 2.1	0.121 ± 0.003

Magnetic hollow micro-nanospheres (ranging from 2 μm to 500 nm) were prepared.

Varying the amount of FeHA (from 1 to 30 wt %), the chemical-physical features of the hybrid beads such as size, surface charge and magnetization can be tailored.

# PLLA-FeHA magnetic micro-nanospheres



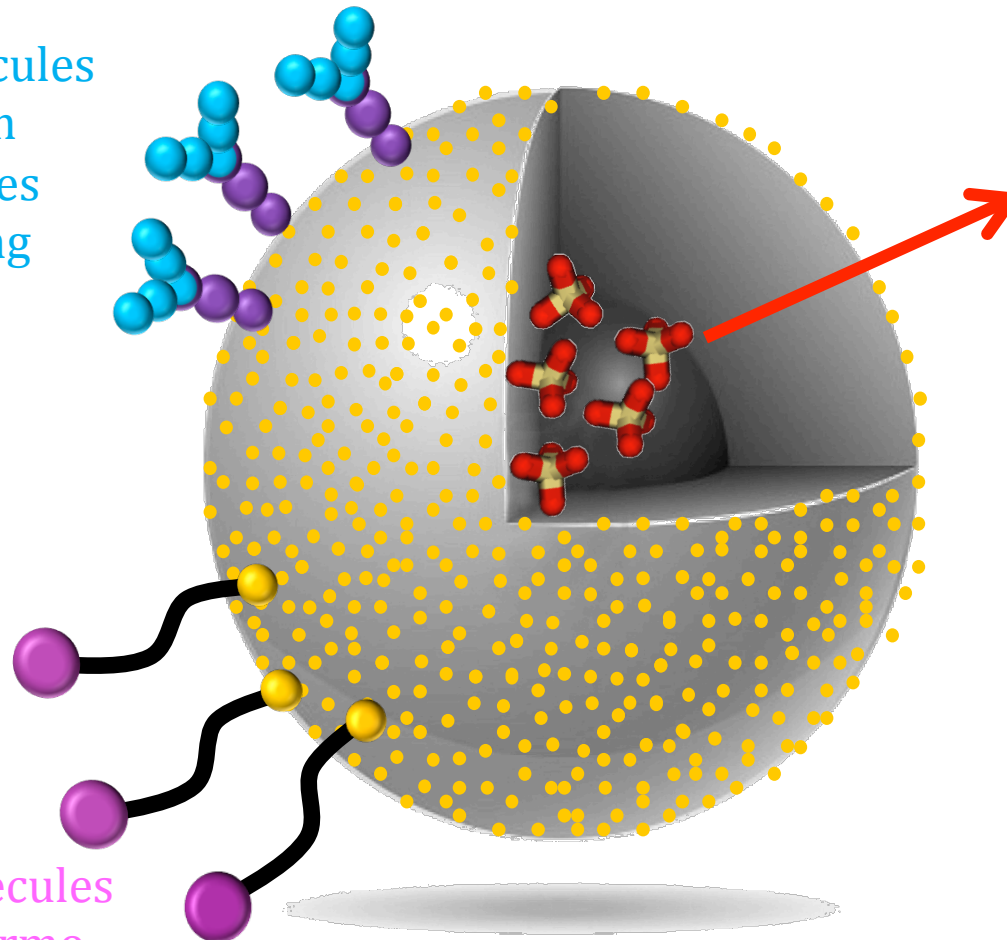
All the samples did not affect the bone marrow mesenchymal stem cells viability or morphology, exhibiting a good level of biocompatibility. The spheres coated with higher amount of FeHA revealed the better cell proliferation than those coated with lower amount

**BONE REGENERATION:** building block for the preparation of new type of scaffold for hard tissue regeneration.

**NANOMEDICINE:** magnetic material for theragnostic applications

# Potential Nanomedical applications

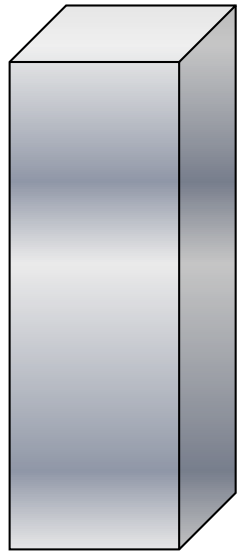
Bioactive molecules  
adsorbed on  
FeHA particles  
(e.g. targeting  
moieties)



Bioactive molecules  
inside the hollow core  
(e.g. therapeutic agents)

Bioactive molecules  
linked by thermo  
ligands

# Bone implants



## Titanium

- Ideal mechanical properties compared with bone
- High metallurgic properties
- Diamagnetic
- Biocompatible
- Bioinert



**NO chemical bond  
with surrounding tissue**

# Bioinspired coatings

## Biomimetic materials

Solutions inspired by bone tissue composition and formation to improve implants

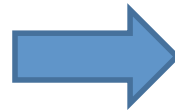
- to reduce healing time and obtain a faster recovery
- to solve complicated situation (like osteoporosis or bone loss)
- to achieve a more durable implant

**Surface is the only part that interacts with living tissue**

Coating



Add new surface property to the material

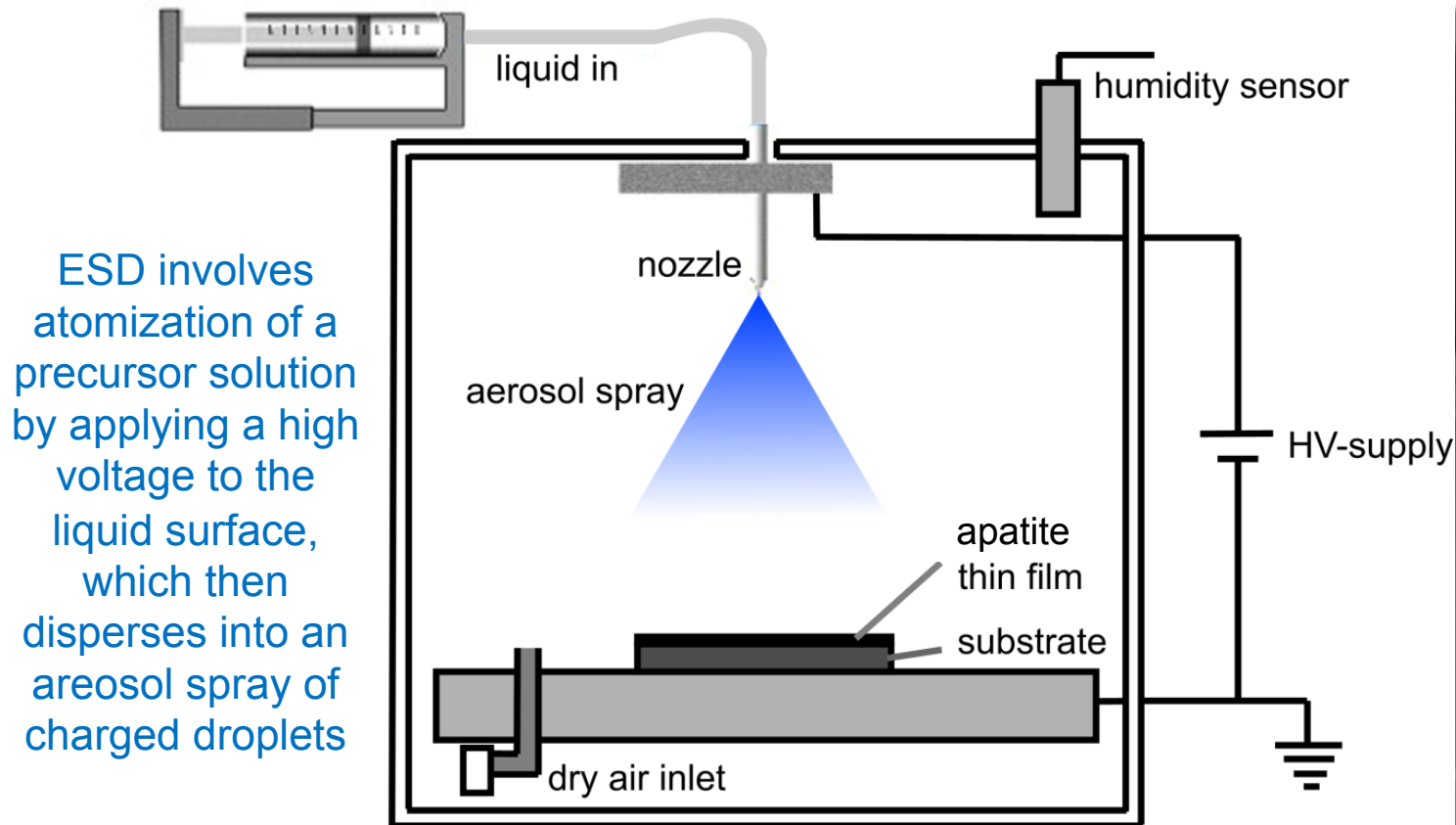


# Coating techniques

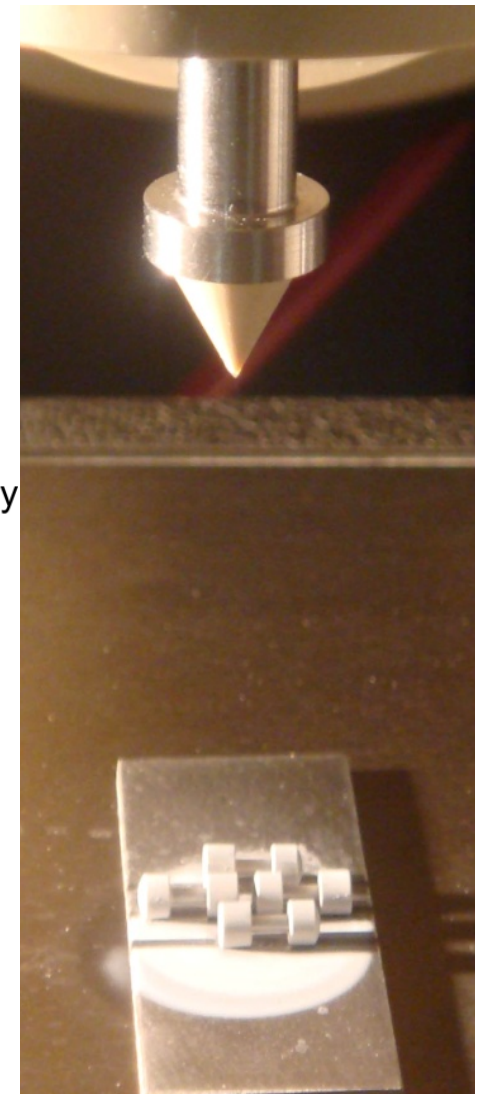
Technique	Coating thickness	Advantage	Disadvantage
Plasma spraying	50–250 $\mu\text{m}$	High deposition rates	Non-uniform coating crystallinity; line of sight technique
RF magnetron sputtering	0.5–5 $\mu\text{m}$	Uniform and dense coating; strong adhesion	Line of sight technique; time consuming; low deposition rates
Electrospray deposition	0.1–5 $\mu\text{m}$	Co-deposition of biomolecules; control over coating composition and morphology	Low mechanical strength; Line of sight technique
Pulsed laser deposition	0.05–5 $\mu\text{m}$	Control over coating chemistry and morphology	Line of sight technique
Hot isostatic pressing	0.2–2 mm	Dense coatings	Thermal expansion mismatch; differences in elastic properties
Ion beam dynamic mixing deposition	0.05–1 $\mu\text{m}$	High adhesive strength	Line of sight technique; requires high sintering temperatures
Sol-gel deposition	<1 $\mu\text{m}$	Coating of complex geometries; low processing temperature	Requires controlled atmosphere processing; expensive raw materials
Dip coating	0.05–0.5 mm	Coating of complex geometries; quick method	Thermal expansion mismatch; high sintering temperatures
Biomimetic deposition	<30 $\mu\text{m}$	Coating of complex geometries; co-deposition of biomolecules	Time consuming; requires controlled pH
Electrophoretic deposition	0.1–2 mm	Uniform coating; coating of complex geometries; high deposition rates	Difficult to produce crack-free coatings; low adhesive strength

de Jong et al., *Pharm Res*, 2008; Leeuwenburgh et al., *Biomaterials*, 2006.

# Electrospray deposition (ESD)



ESD involves atomization of a precursor solution by applying a high voltage to the liquid surface, which then disperses into an aerosol spray of charged droplets

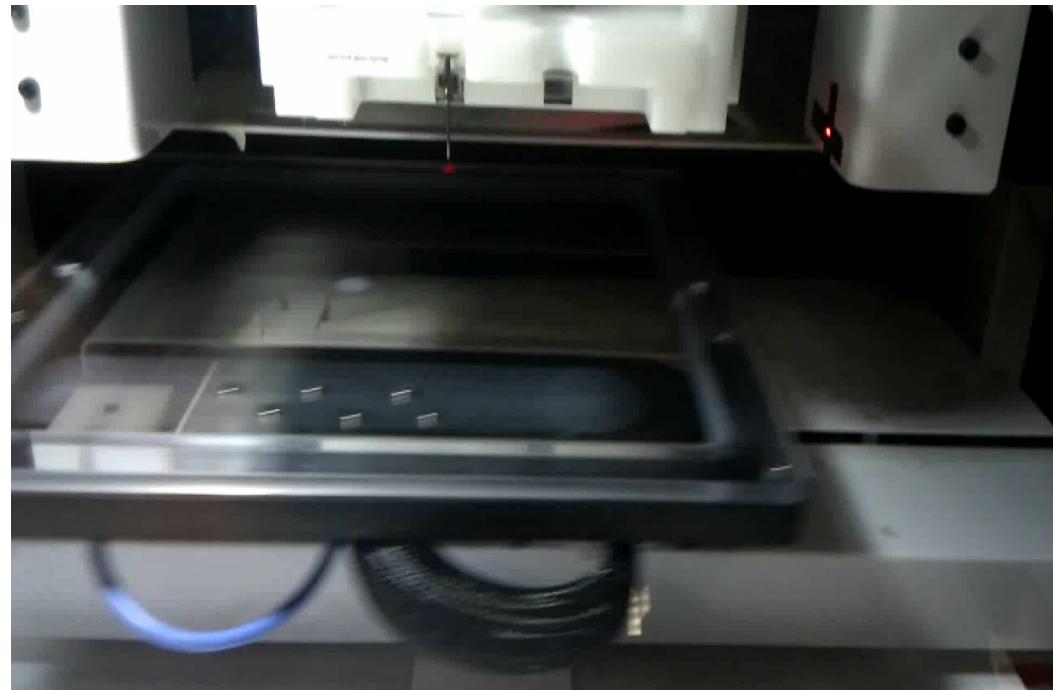


**Control over: quantity, thickness and coated area**

Leeuwenburgh et al., *J Biomed Mater Res A*, 2005; Iafisco et al., *Adv Eng Mat*, 2012

# Electrospray deposition (ESD)

Usually a spherical droplet is formed at the tip of nozzle when pumping a solution, but when a high voltage is applied, this droplets transforms into a conical shape and fans out to form a spray of highly charged droplets



Leeuwenburgh et al., *J Biomed Mater Res A*, 2005; Iafisco et al., *Adv Eng Mat*, 2012

# Electro spray deposition (ESD)

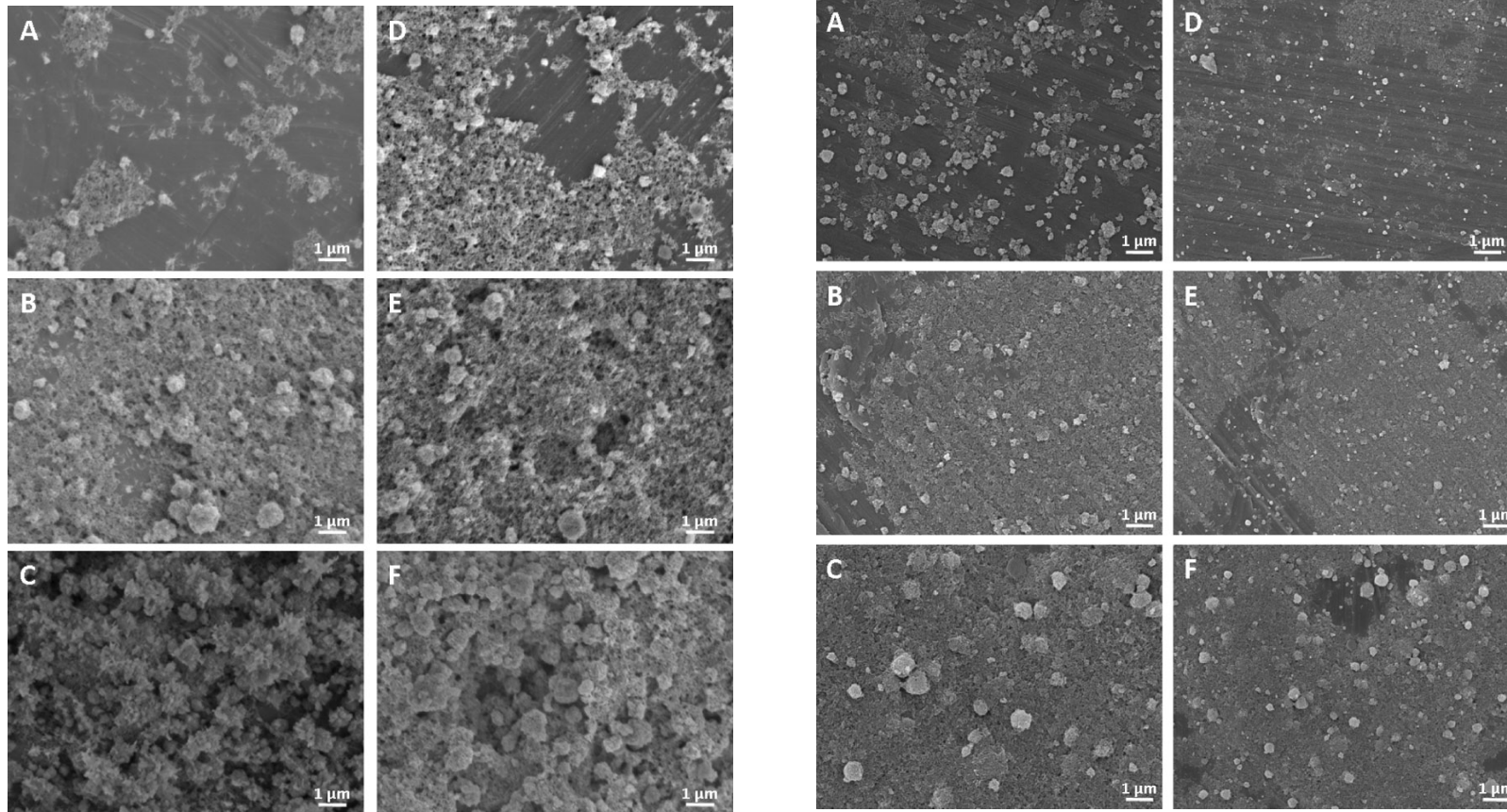


Table 2. ESD parameters for deposition of HA coatings evaluated in this work.

Nozzle-to-substrate distance [mm]	20	40	
Relative humidity in the deposition chamber [%]	20	40	
Deposition time [min]	5	15	30

Relative humidity did not show a significant effect on the morphology of the coating, whereas the nozzle-to-substrate distances affected the residence time of the droplets and hence the homogeneity of the deposited layers

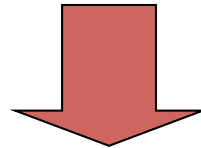
Iafisco et al., *Adv Eng Mat*, 2012

# Functionalization of HA

The surface functionalization of HA nanocrystals with bioactive molecules makes them able to transfer information to and to act selectively on the biological environment. In particular, the functionalization with drugs could represent a local treatment for bone diseases by direct application of the modified HA.

**Biocompatibility**

(HA nanocrystals)



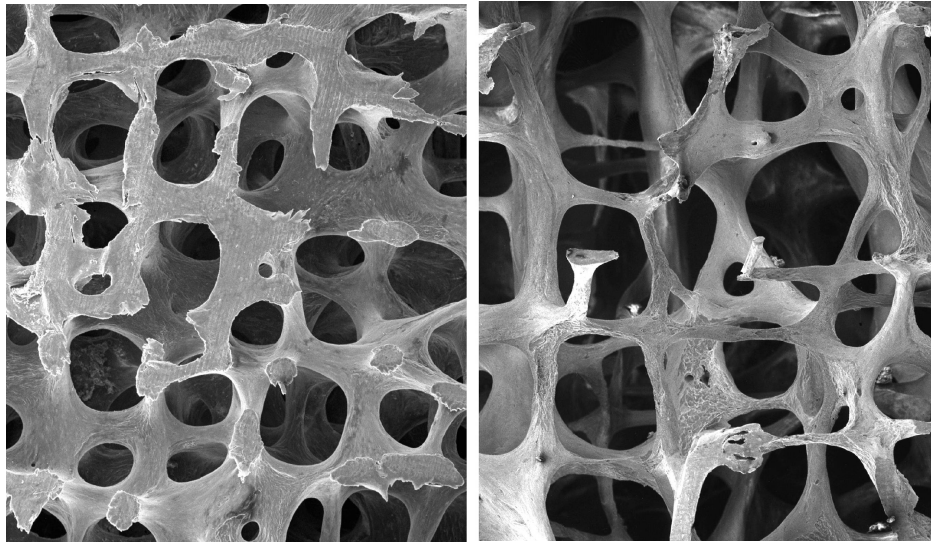
**Bioactivity**

(HA nanocrystals/biomolecules)

lafisco et al., *Langmuir*, 2008; lafisco et al., *Coll Surf B*, 2010; lafisco et al., *Dalton Trans*, 2011; lafisco et al., *J. Inorg. Biochem.*, 2012

# Osteoporosis

A condition of skeletal fragility characterized by compromised bone strength predisposing to an increased risk of fracture

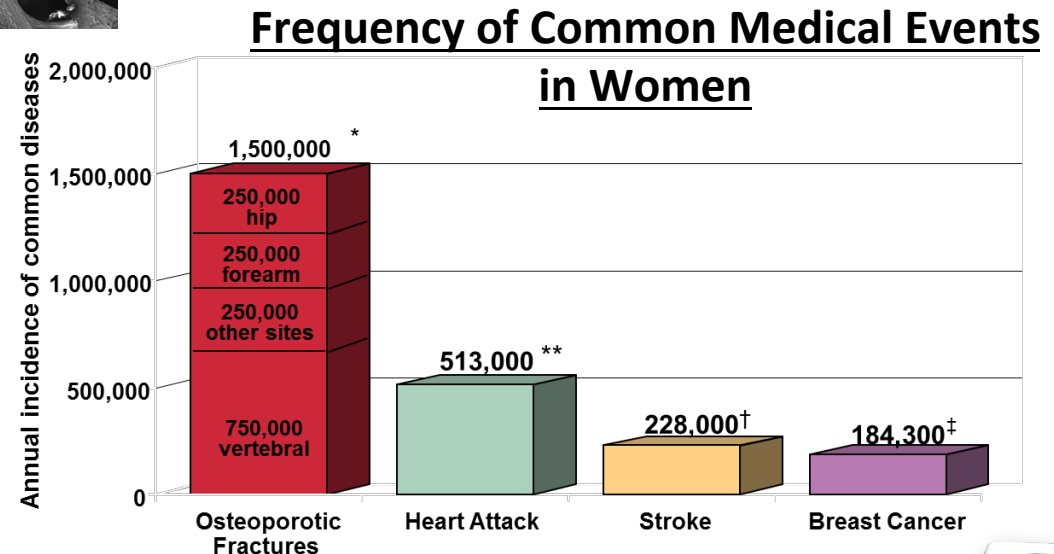


Comparison of normal and osteoporotic bone architecture

## Osteoporotic Bone Tissue

- Bone turnover altered
- Compromised mechanical properties
- Degenerative

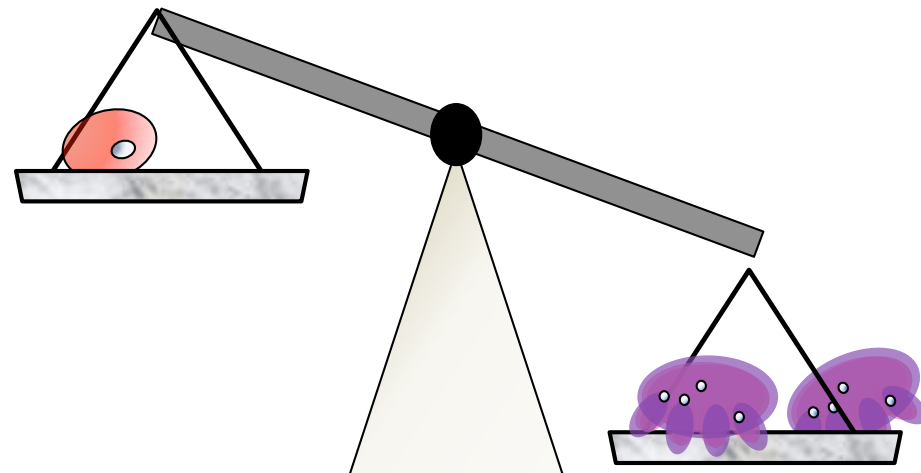
Russell et al., *Osteoporosis International*, 2008



## Pathologic condition: Osteoporosis

- It is diagnosed to over 25 million new people each year.
- It is responsible for one and a half million fractures each year and costs \$15 billion for fracture care.
- In Europe, the disability cost due to osteoporosis is greater than that caused by cancers
- It has been treated for 40 years with bisphosphonate based drugs

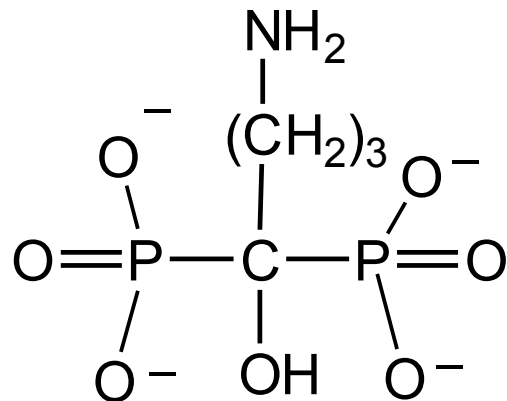
*Osteoporosis results from an imbalance between osteoblast and osteoclast activity.*



<http://www.brsoc.org.uk>

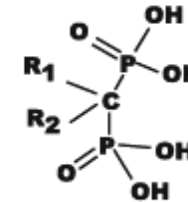
# Bisphosphonates

Chemical structure of bisphosphonates used in humans.

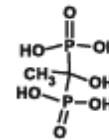


**ALENDRONATE**

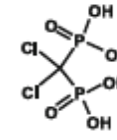
## Bisphosphonate Structures



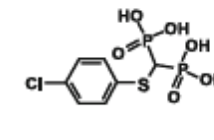
### Non N-BPs



Etidronate

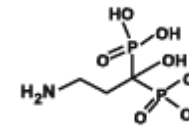


Clodronate

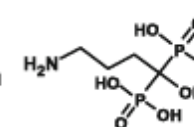


Tiludronate

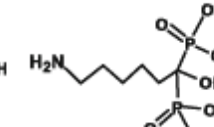
### Alkyl-amino BPs



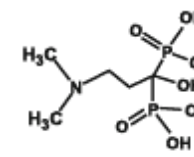
Pamidronate



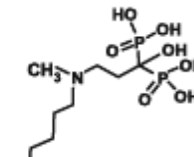
Alendronate



Neridronate

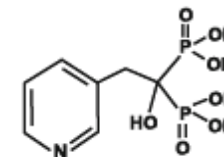


Olpadronate

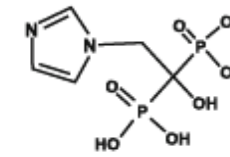


Ibandronate

### Heterocyclic N-BPs

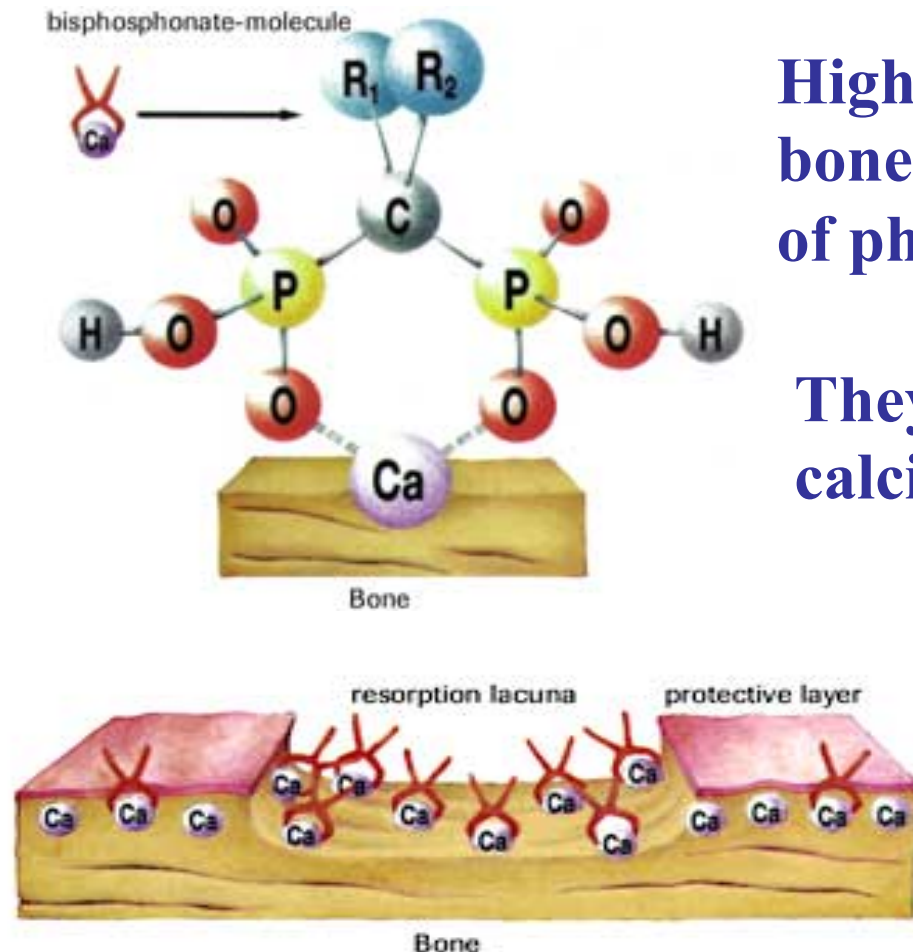


Risedronate



Zoledronate

# Bisphosphonates



High ability to chelate  $\text{Ca}^{2+}$  ions of bone tissue thanks to the large affinity of phosphonates groups for this.

They are physiological regulator of calcification and bone resorption

Paget's bone disease

Osteoporosis

Fibrous dysplasia

Myeloma

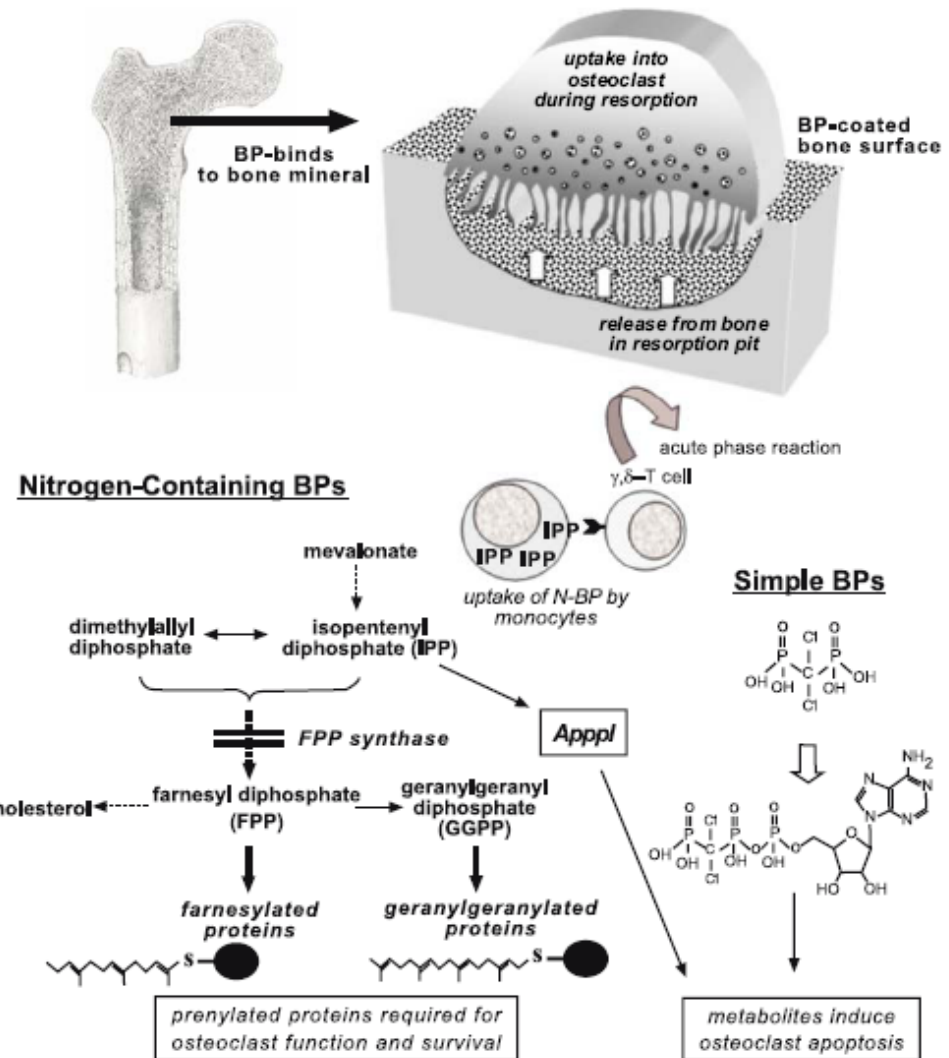
Bone metastases

# Bisphosphonates

After binding to bone mineral, the drugs are internalized into bone-resorbing osteoclasts by endocytosis.

Simple BPs are metabolized in the osteoclast cytosol to ATP analogues that induce osteoclast apoptosis.

N-BPs inhibit FPPS, thereby preventing the prenylation of small GTPase proteins essential for the function and survival of osteoclasts.

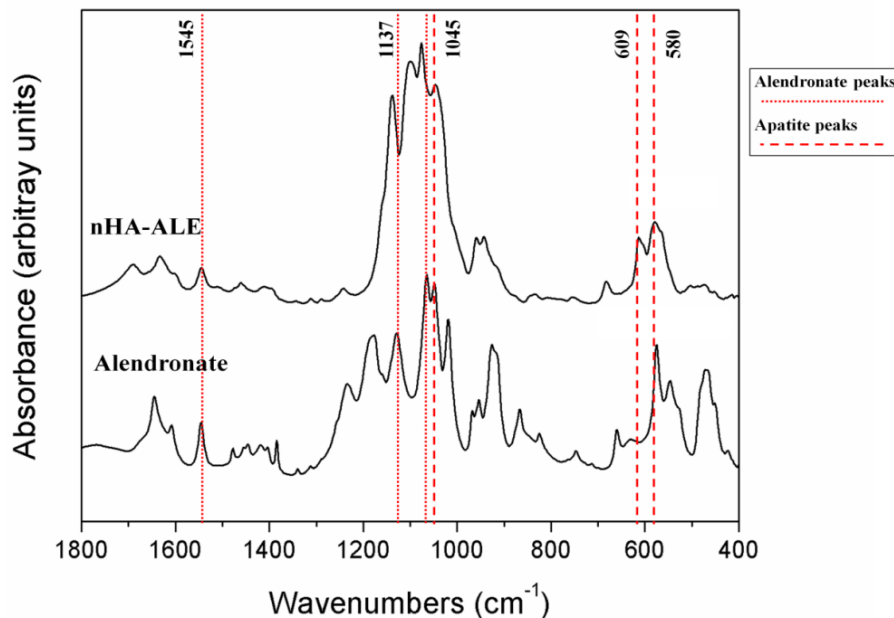
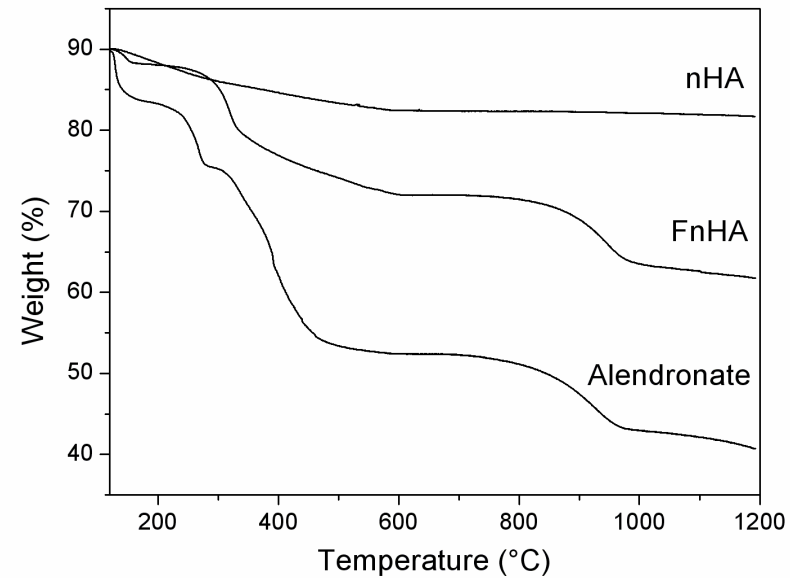
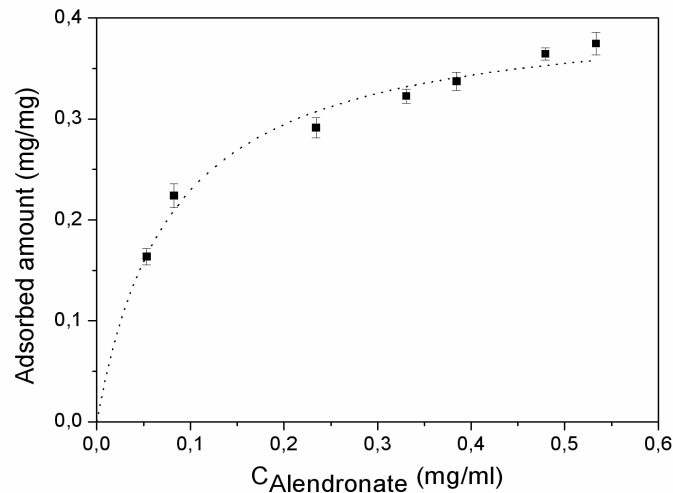


## Side effects

Osteonecrosis of the jaw  
Gastric-digestive associated pathologies

Russell et al., *Osteoporosis International*, 2008

# Functionalization of apatite with alendronate

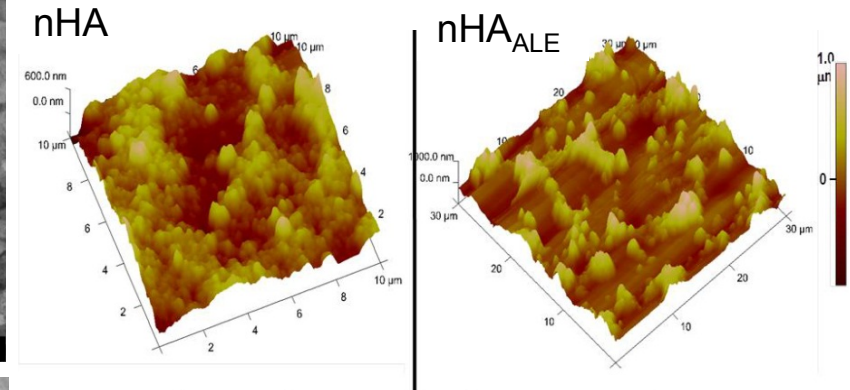
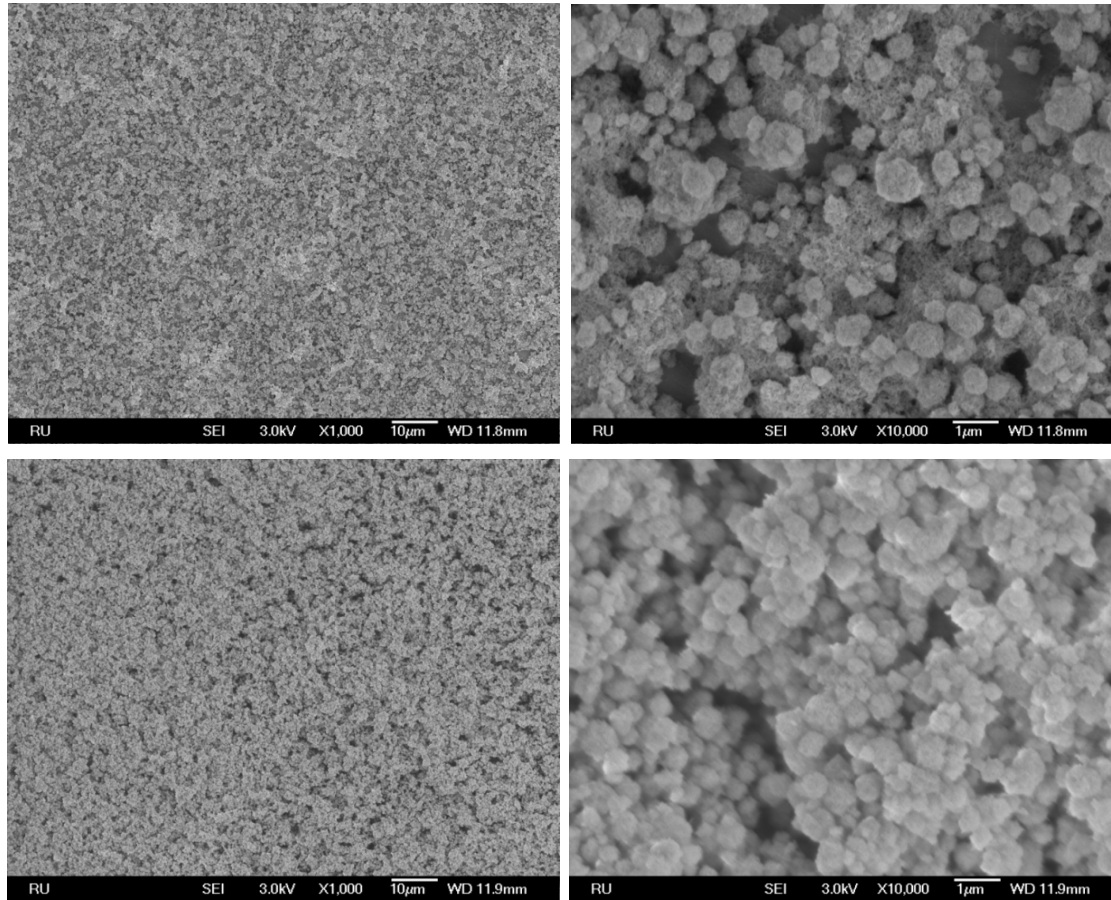


The amount of alendronate attached to HA was calculated to be 29.5 wt% which corresponds to a drug surface immobilization on HA of about 0.42 mg/mg.

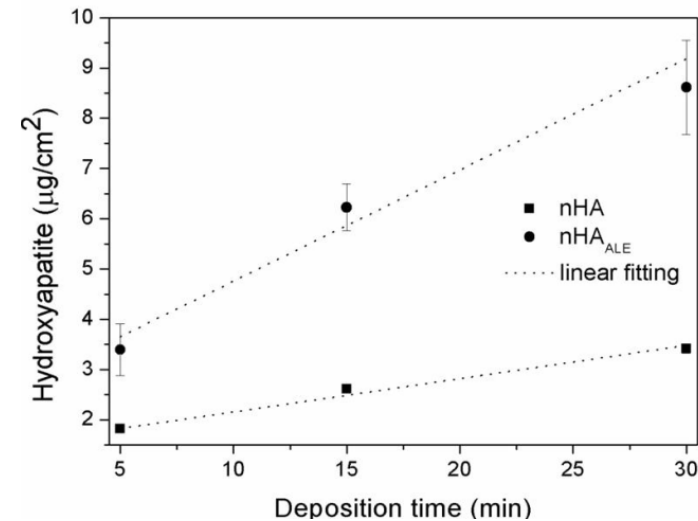
FTIR confirmed the strong interaction of alendronate to HA by the chemical link of phosphonate groups with the Ca ions of HA and by the formation of hydrogen bonds of the alendronate amino group with the HA surface.

Bosco et al., *submitted*

# Coatings of Apatite functionalized with alendronate



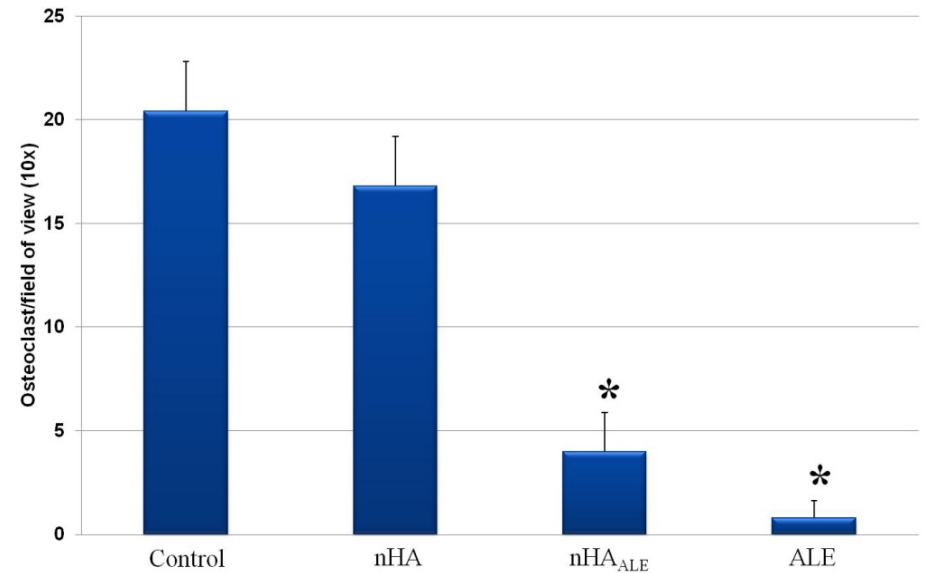
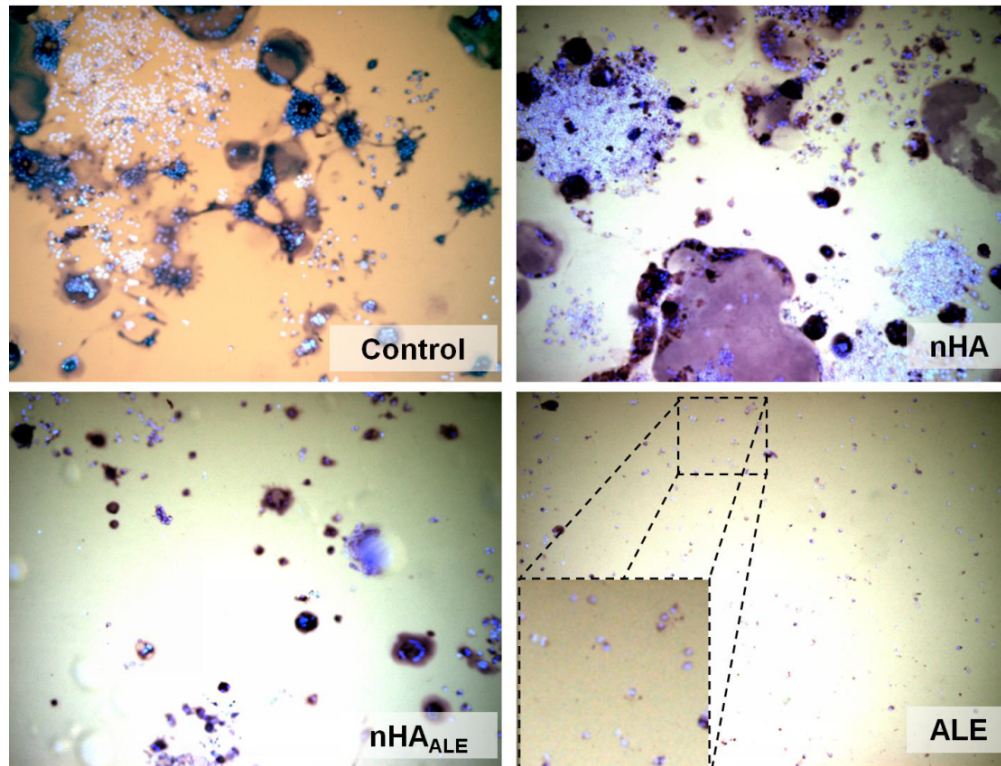
Coating	Thickness [nm]	Ra [nm]
nHA	569.89 ± 24.73	234.80 ± 46.55
nHA <sub>ALE</sub>	771.46 ± 77.05	289.67 ± 11.93



Ti disks coated with:	O (%)	Na (%)	Ti (%)	N (%)	C (%)	P (%)	Ca (%)	Ca/P
Alendronate	35.9	5.2	0.8	4.6	44.0	9.5	-	
nHA	46.9	-	-	-	21.8	13.1	18.2	1.39
nHA <sub>ALE</sub>	47.1	-	-	0.8	19.8	14.7	17.6	1.20

Bosco et al., *submitted*

# Coatings of Apatite functionalized with alendronate



Quantification of osteoclasts per field of view. Osteoclasts have been counted only in presence of 3 or more nuclei and TRAP positive membrane. Variance analysis has been performed (ANOVA)

Effect of alendronate-hydroxylapatite on osteoclasts. (A) Control group, (B) incorporation of nHA, (C) addition of FnHA and (D) effect of Alendronate. TRAP and DAPI staining, 10x magnification, day 4, 2000 cells/cm<sup>2</sup>

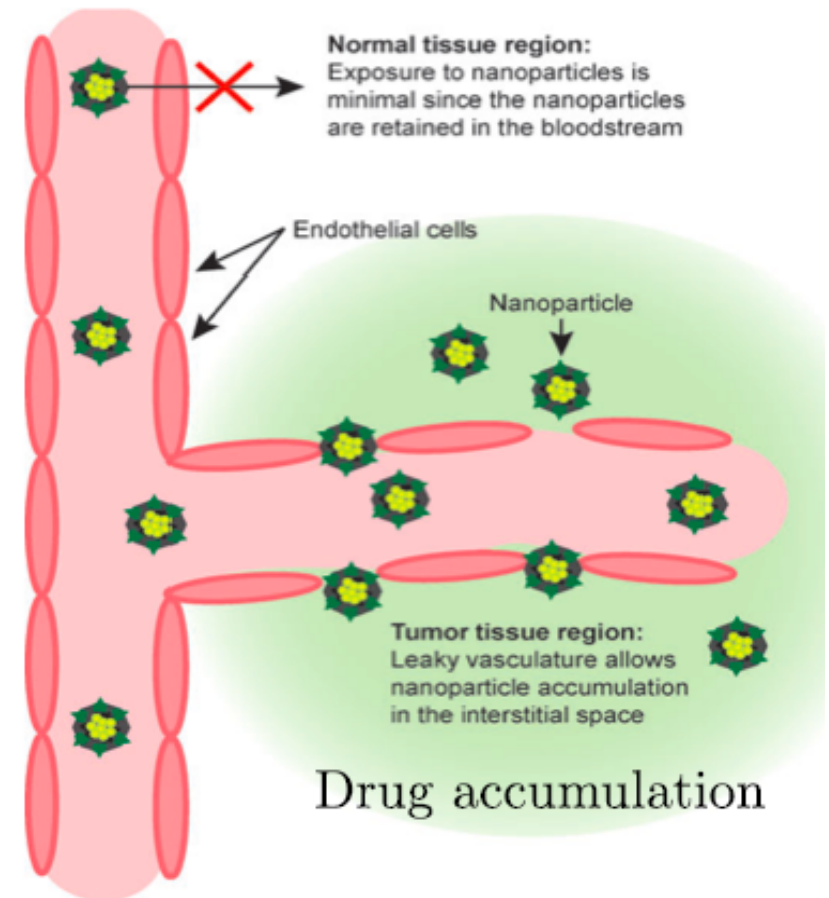
Bosco et al., *submitted*

# Applications

## Why nanoparticles (NPs) as injectable drug carriers?

Nano dimension allows the prolonged circulation in the blood stream escaping the capture from macrophages and the accumulation at the tumor site by “passive targeting” through the enhanced permeability and retention effect

Increase the specificity of the drug and thus, reducing its side effects



Iafisco et al. *Nanoscale*, 2012; Iafisco et al., *J Inorg Biochem*, 2012

# Applications

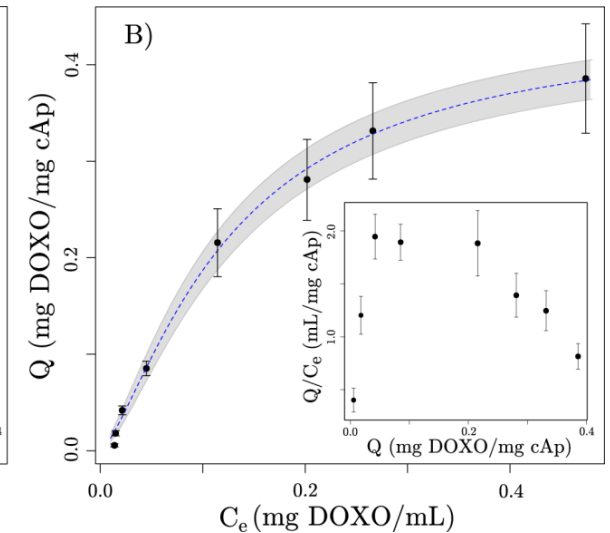
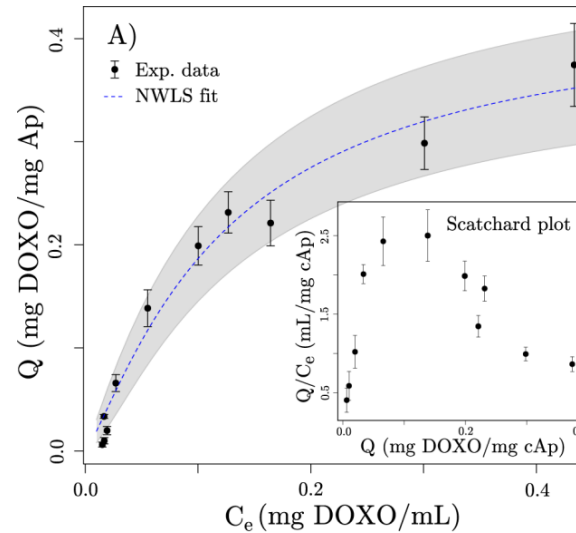
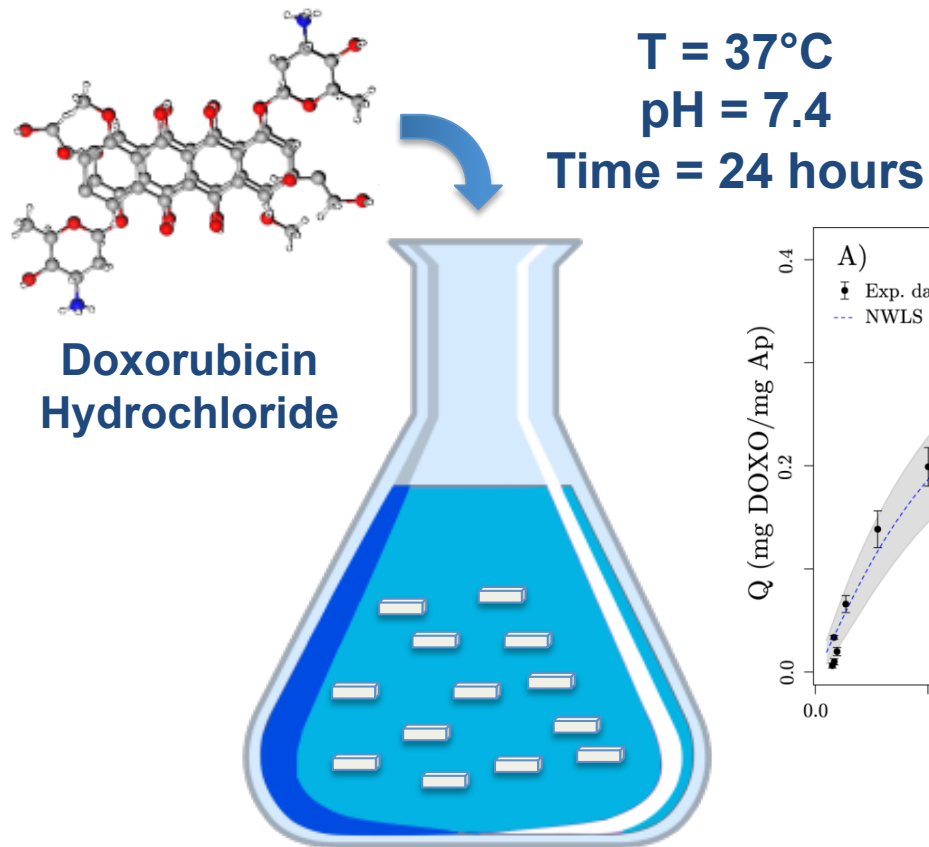
## Why apatite as nanocarriers?

- Favorable biodegradability and biocompatibility
- Higher degradability and lower toxicity than silica, quantum dots, carbon nanotubes, or metallic magnetic particles
- Higher stability than liposomes, allowing a more controlled and predictable drug delivery
- Low production costs and excellent storage properties (not easily subjected to microbial degradation)
- The stability is pH-dependent: **Stable** at pH=7.4 but **Degradable** at pH=5.0 (cancerous region and lysosomes inside the cells) that allows the drug release

lafisco et al. *Langmuir*, 2008; lafisco et al. *J Mat Chem*, 2009;  
lafisco et al. *Nanoscale*, 2012; lafisco et al., *J Inorg Biochem*, 2012

# Drug loading

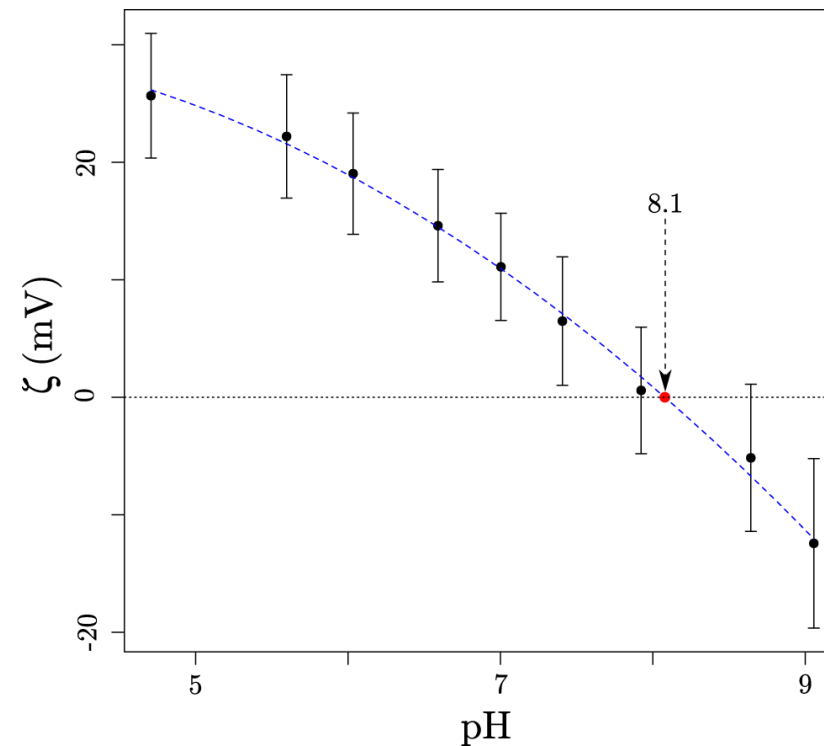
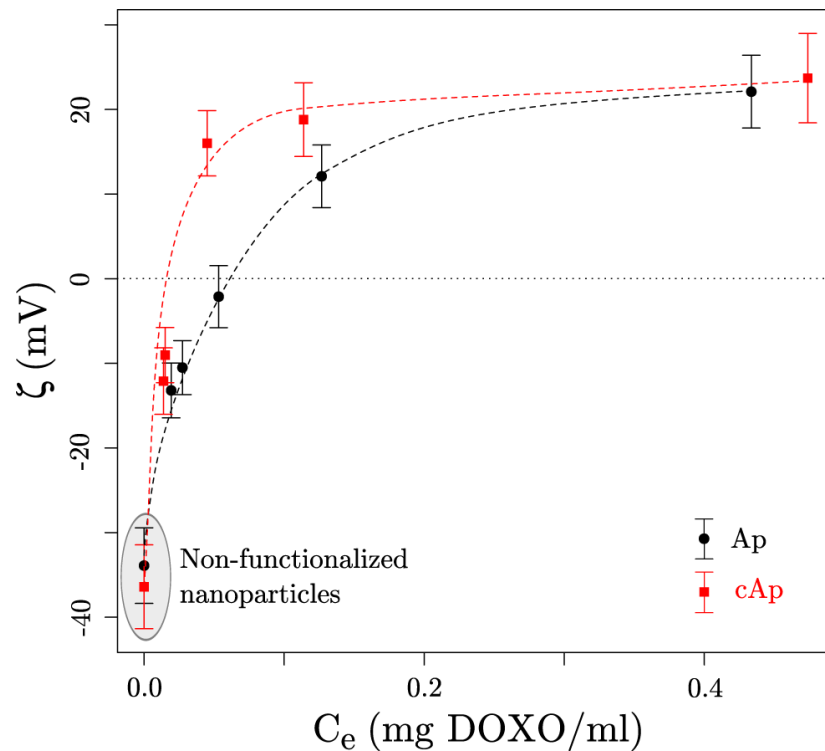
## Isothermal adsorption of Doxorubicin (dimer) on Ap and cAp



**$Q_{\text{max}}$  is around 0.4 mg Dox/mg of apatite**

Rodriguez-Ruiz et al., *Langmuir*, 2013

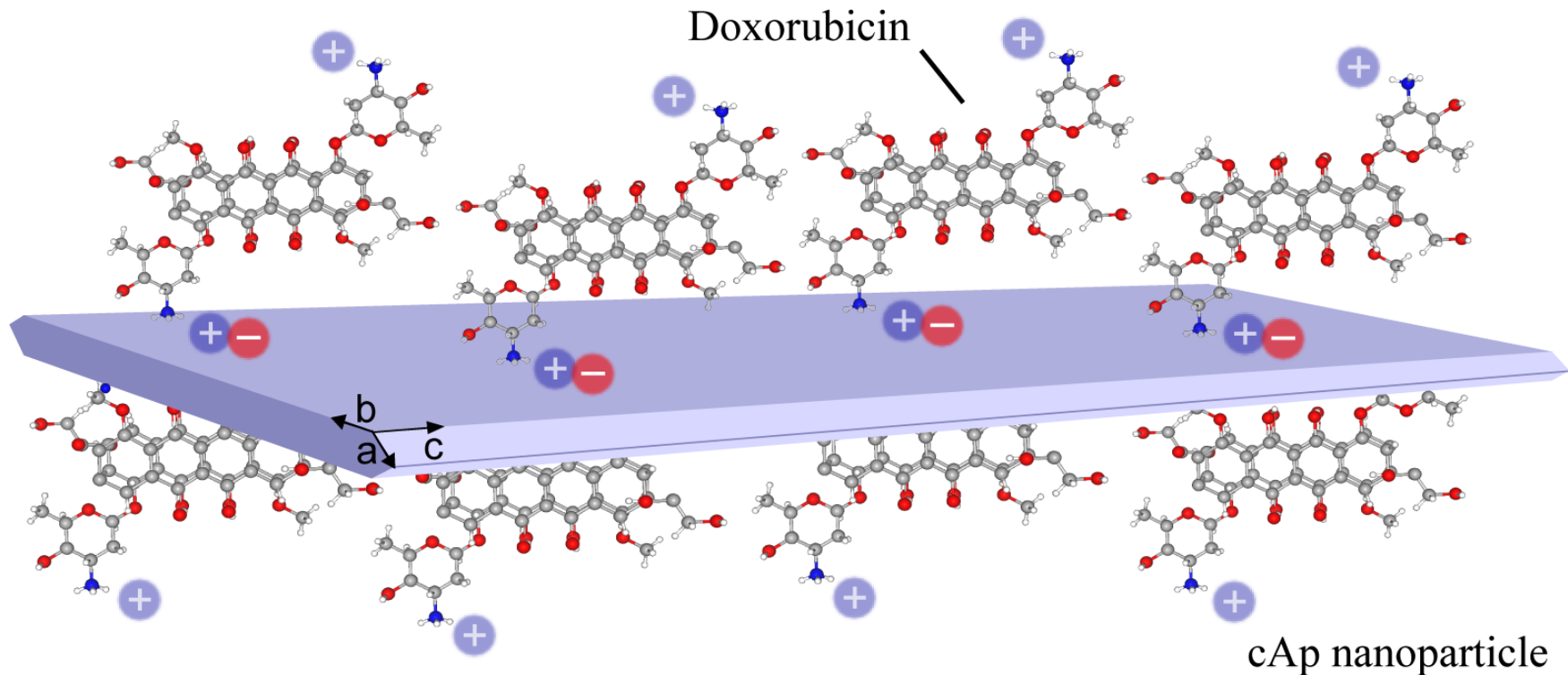
# Drug-Nanocrystals interaction



- $\zeta$  increases with Dox coverage reaching positive values
- $\zeta$  decreases when increasing the pH. Deprotonation of  $-\text{NH}_3^+$  groups

Rodriguez-Ruiz et al., *Langmuir*, 2013

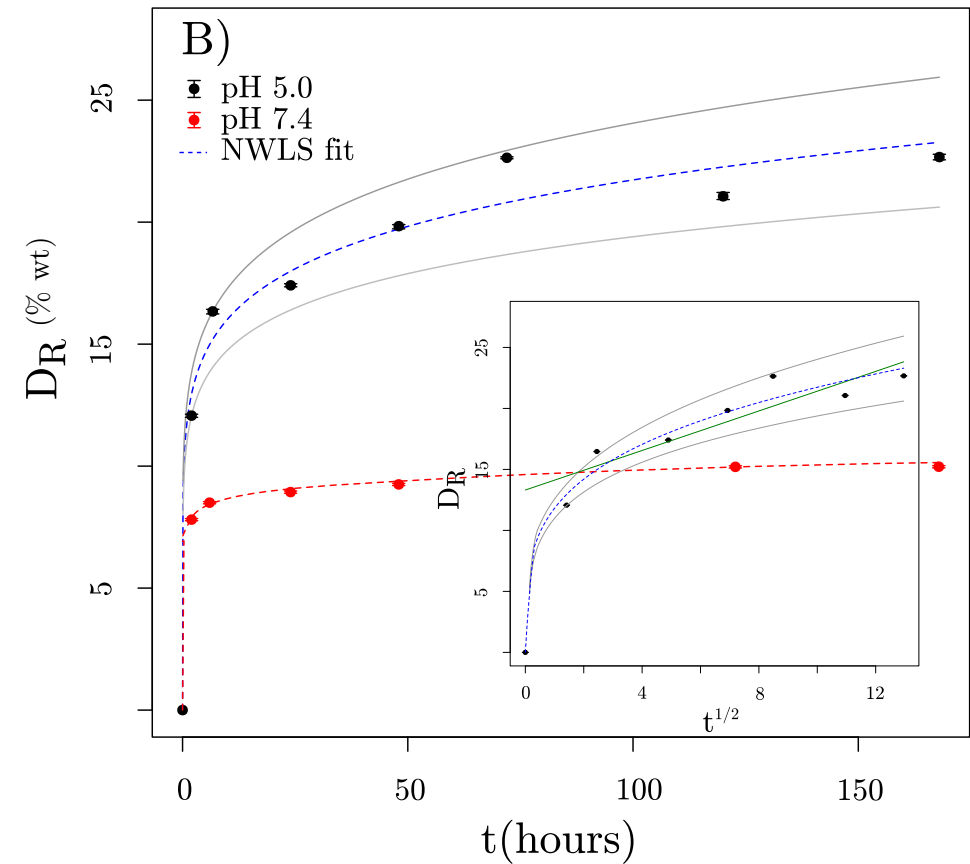
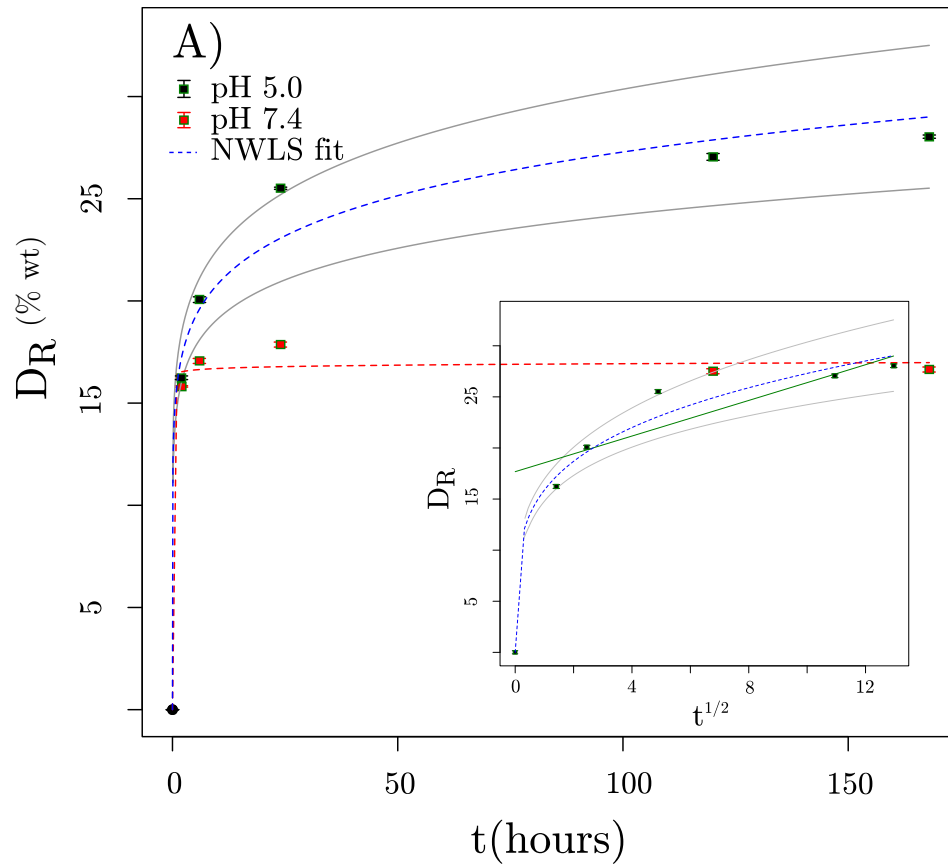
# Drug-Nanocrystals interaction



**DOXO is attached as a dimer by means of a positively-charged amino group which electrostatically interacts with negatively charged surface groups of apatite**

Rodriguez-Ruiz et al., *Langmuir*, 2013

# Drug release



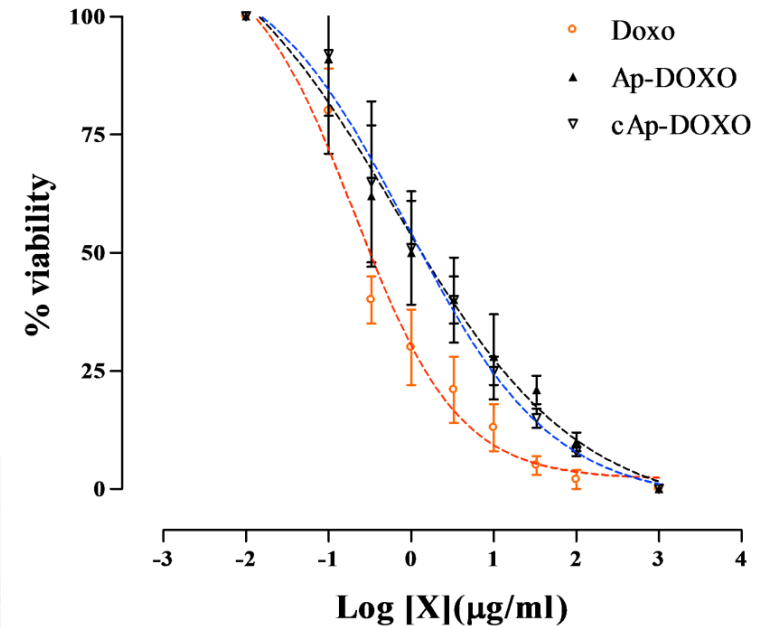
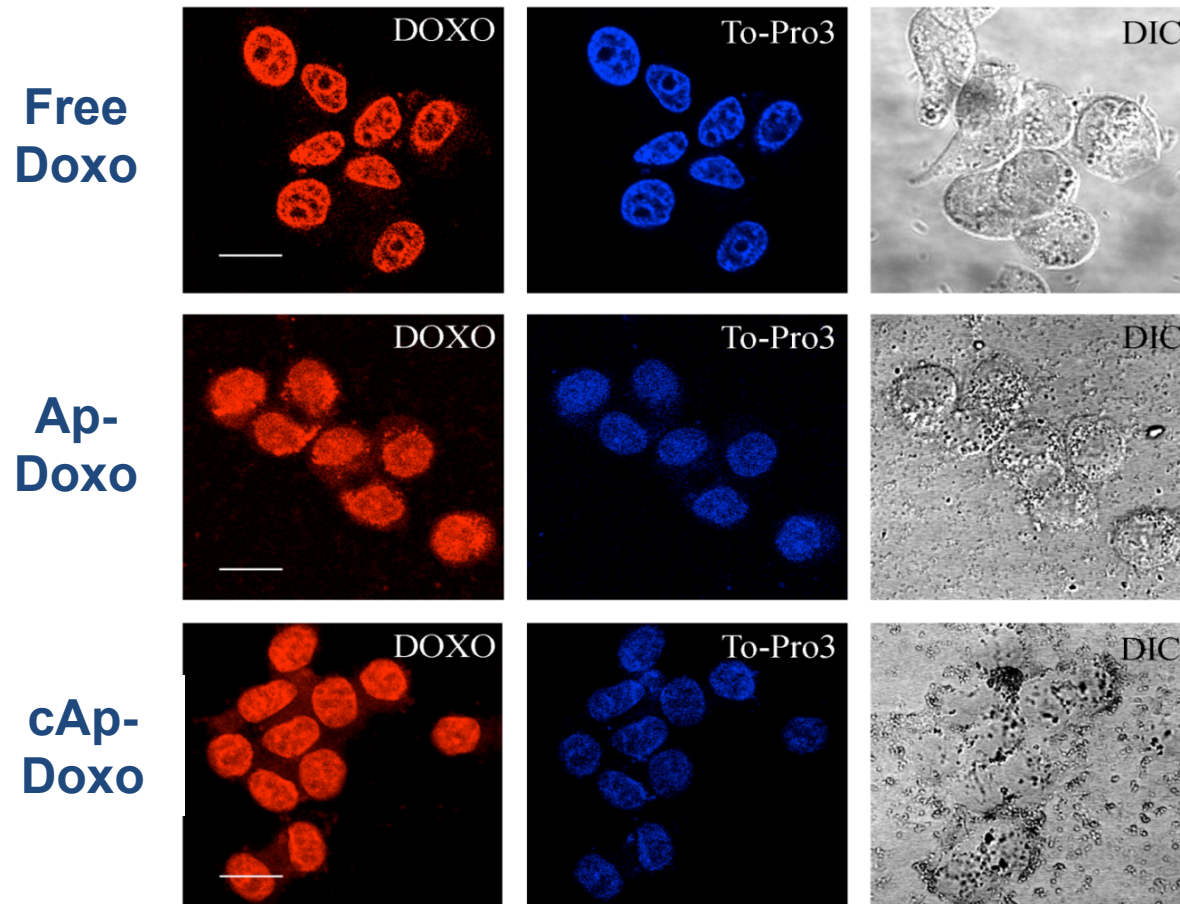
**Higher release of DOXO at pH 5.0 than at pH 7.4**

Rodriguez-Ruiz et al., *Langmuir*, 2013

NIS colloquium "Advances in biomaterials: combining simulations and experiments", Turin, November 29, 2013



# In vitro assay

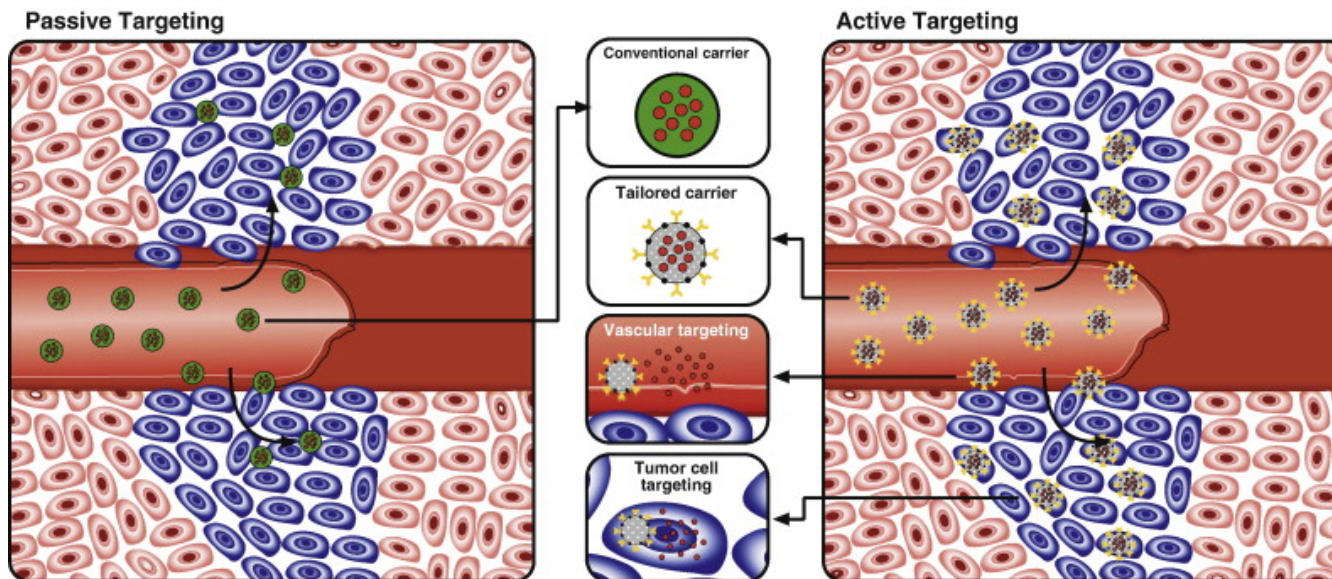
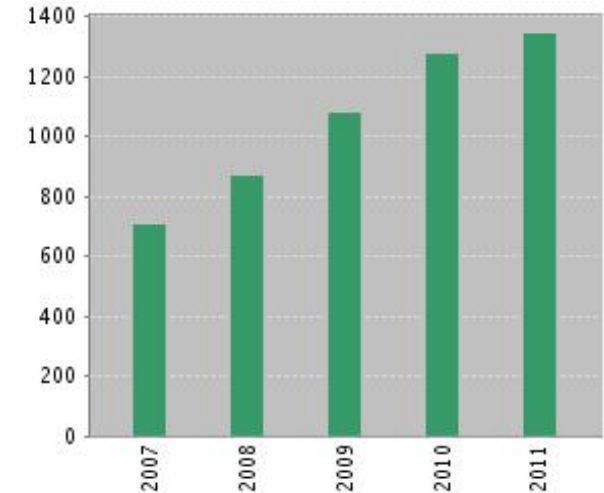


- Both apatites were internalized within GTL-16 human carcinoma cells and release Doxo which accumulated in the nucleus
- Apatite-Doxo exerted cytotoxic activity with the same efficiency of the free drug

Rodriguez-Ruiz et al., *Langmuir*, 2013

# The fundamental role of targeting

- NPs dimension allows the prolonged circulation in the blood stream escaping the capture from macrophages and the accumulation at the tumor site by “passive targeting” through the enhanced permeability and retention effect
- The specifically active targeting mediated by affinity ligands may provide additional or alternative delivery mechanisms to EPR

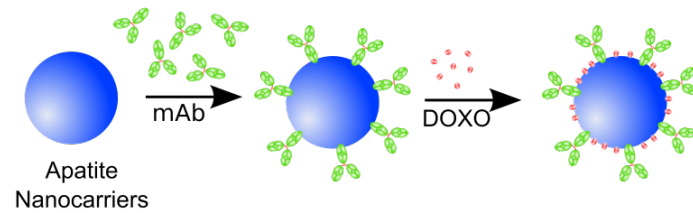


- Folic acid
- Transferrin
- Integrins
- Monoclonal antibodies

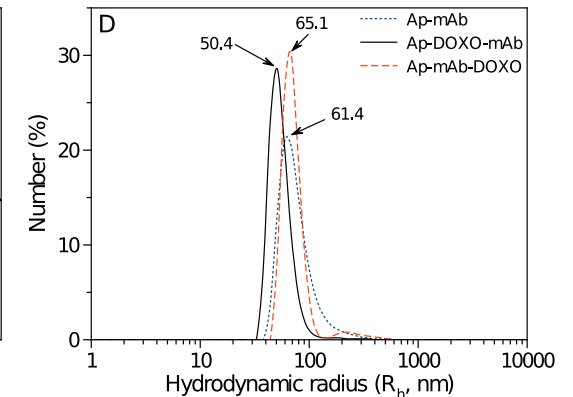
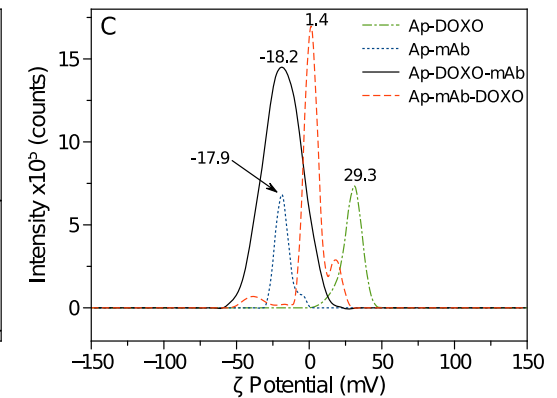
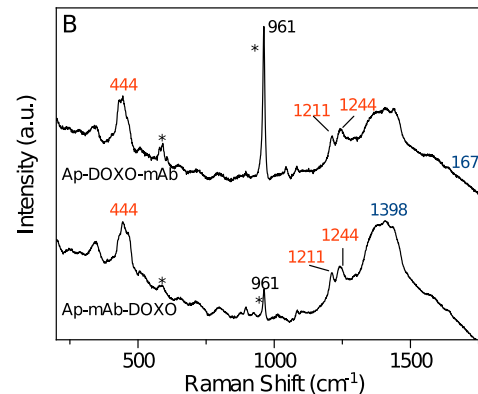
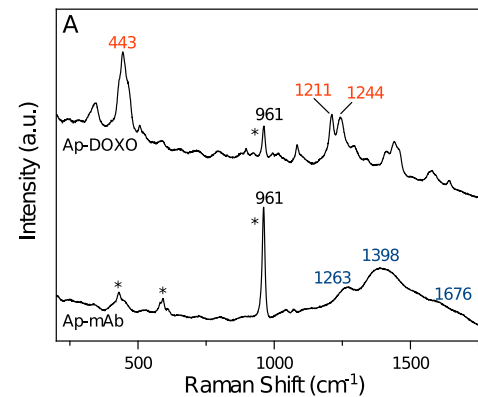
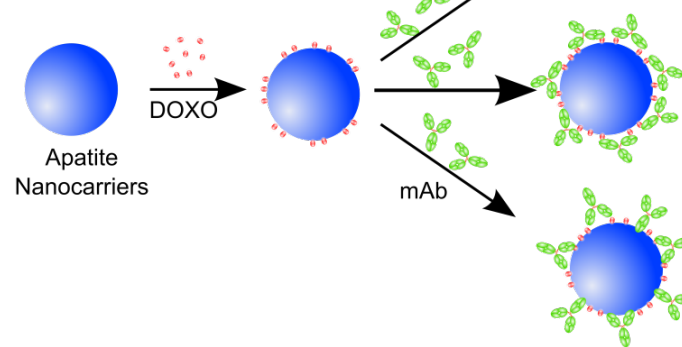
# Cell Surface Receptor Targeted Apatite

Functionalization with doxorubicin (DOXO) and the DO-24 monoclonal antibody (mAb) directed against the Met/Hepatocyte Growth Factor receptor (Met/HGFR), which is over-expressed on different types of carcinomas and represents a useful tumor target.

Method 1: Ap + mAb + DOXO



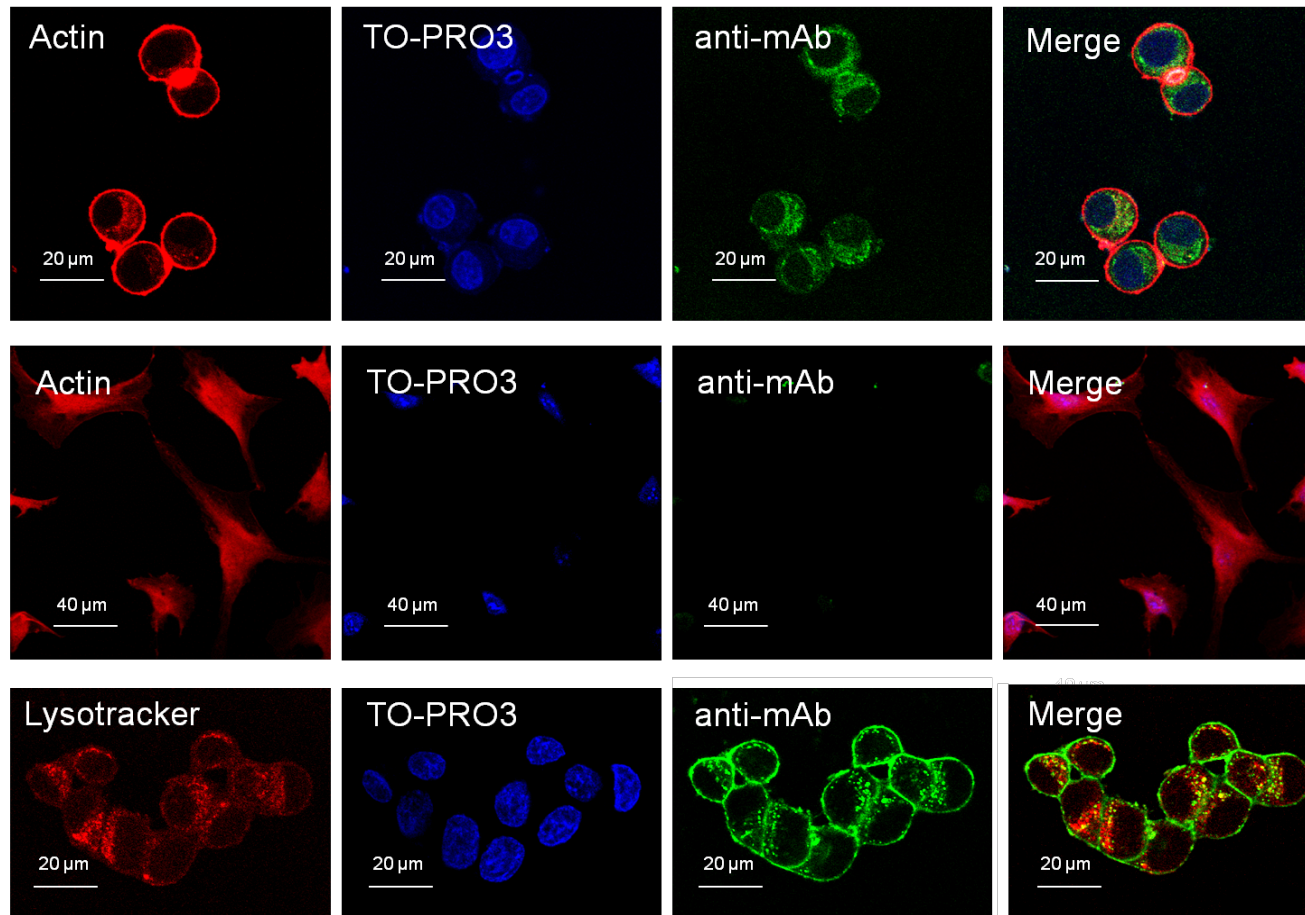
Method 2: Ap + DOXO + mAb



At pH 7.4 no significant release of mAb and DOXO was detected, whereas about the 80% of the bound DOXO, as well as of the mAb, were released upon 3 days at pH 5.0

lafisco et al., *Small*, 2013

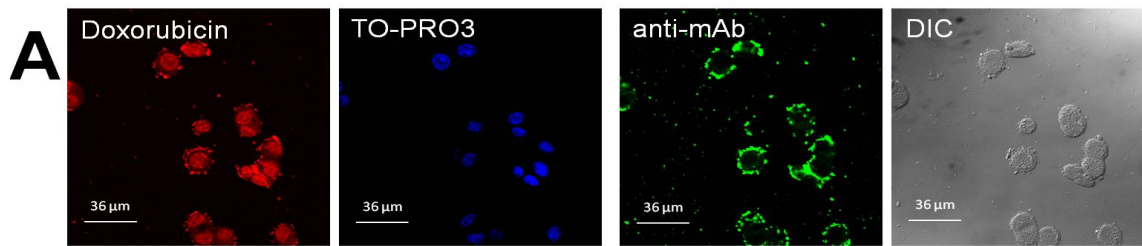
# Cell Surface Receptor Targeted Apatite



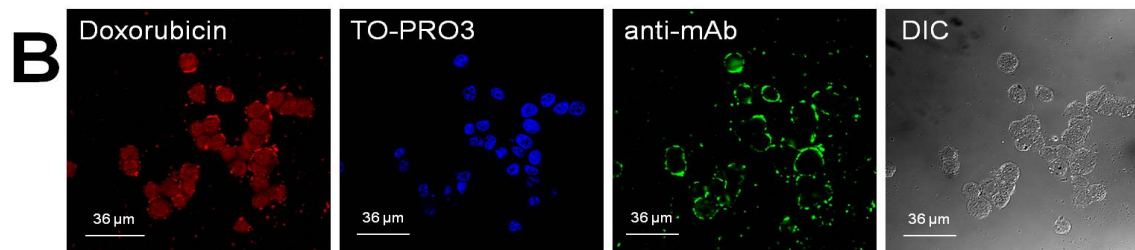
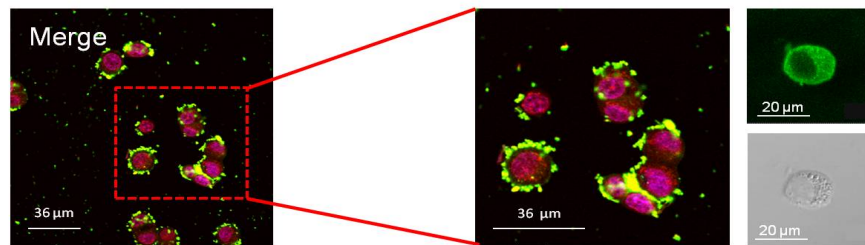
Analysis of the specificity of the interaction of the DO-24 mAb loaded Ap nanoparticles (Ap-mAb) with cells and of their internalization by confocal microscopy. Met<sup>+</sup> GTL-16 cells (top row) and Met<sup>-</sup> NIH-3T3 fibroblasts (medium row) were incubated with nanoparticles at 37 °C for 3 h.

Iafisco et al., *Small*, 2013

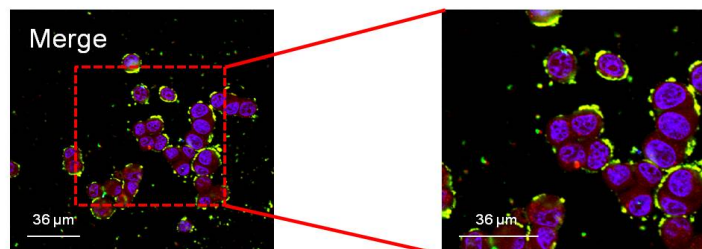
# Cell Surface Receptor Targeted Apatite



Internalization in GTL-16 cells by confocal microscopy. Cells were incubated with Ap-mAb-DOXO (A) or Ap-DOXO-mAb (B) at 37°C for 3h, washed, fixed, permeabilized and saturated. Nanoparticles are visualized in green (staining with FITC-labeled anti-mouse IgG), nuclei in blue (TO-PRO3) and DOXO in red.

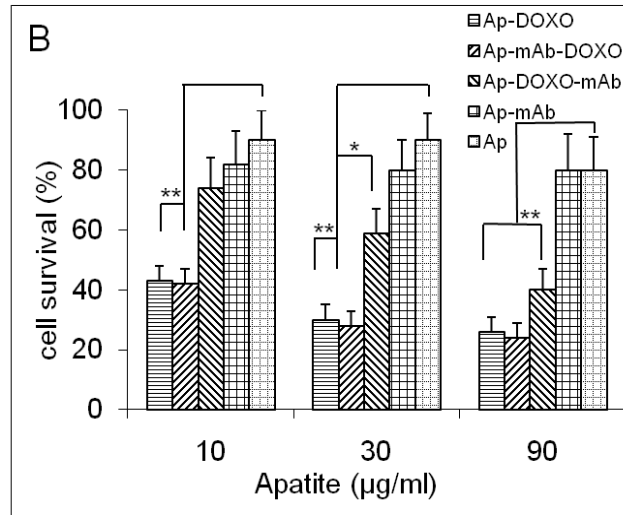
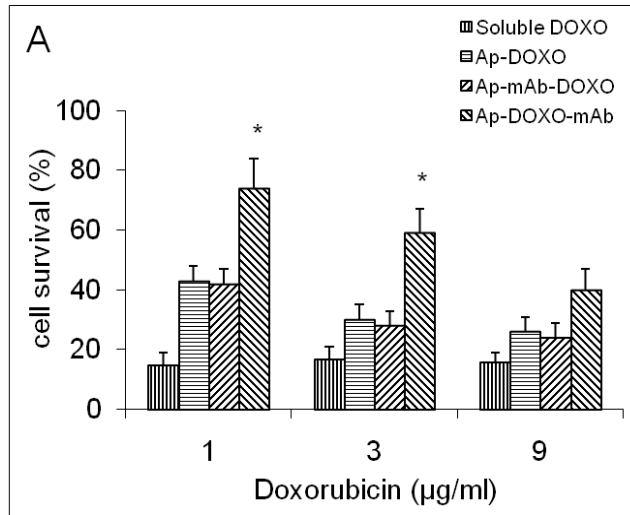


Green fluorescence revealing mAb-loaded NPs at the cell surface or in its proximity and red corresponding to DOXO inside the cells. DOXO is mainly localized in the nucleus when using Ap-mAb-DOXO assemblies, it is equally distributed within the whole cells when then Ap-DOXO-mAb are employed. Therefore, the Ap-mAb-DOXO system was found to bind at the cell surface with higher efficiency and to release DOXO in the nucleus more efficiently



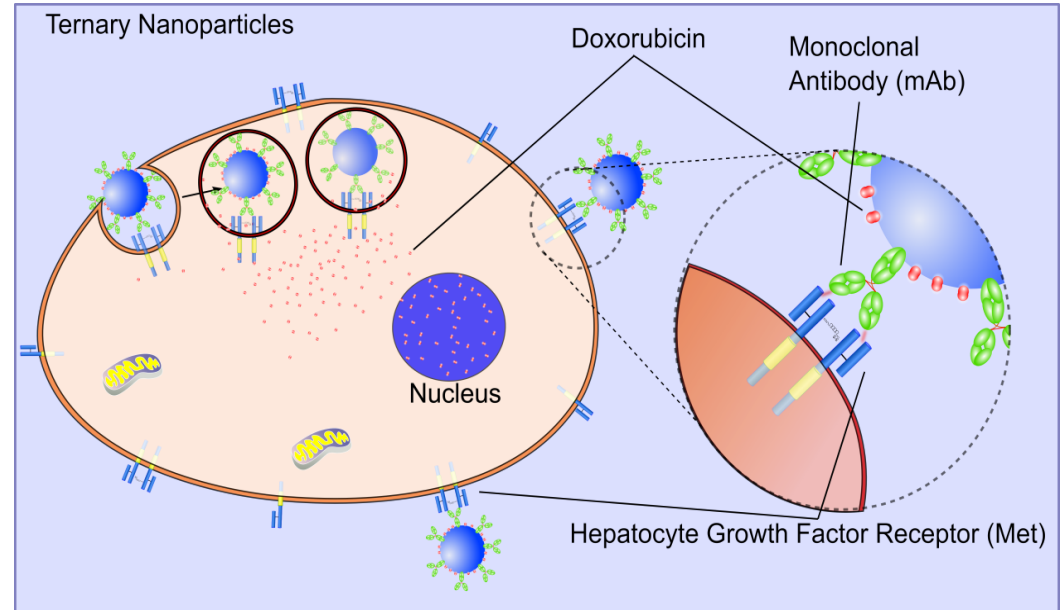
Iafisco et al., *Small*, 2013

# Cell Surface Receptor Targeted Apatite



Cytotoxic activity of the differentially functionalized nanoparticles on GTL-16 cells.

Functionalized nanoparticles specifically bound to and were internalized in cells expressing the receptor (GTL-16) but not in the ones that do not express it (NIH-3T3). Moreover they discharged DOXO in the targeted GTL-16 cells that reached the nucleus and displayed cytotoxicity as assessed in an MTT assay.



Iafisco et al., *Small*, 2013

# Acknowledgements

## **ISTEC-CNR, Italy**

Dr. Anna Tampieri, Dr. Monica Sandri, Dr. Silvia Panseri, Dr. Alessio Adamiano

## **Laboratorio de Estudios Cristalográficos, CSIC-UGR, Granada, Spain**

Prof. Jaime Gómez-Morales, Dr. Josè-Manuel Delgado-Lopez

## **Radboud University Nijmegen Medical Center, The Netherlands**

Prof. John Jansen, Prof. Sander Leewenburgh, Ruggero Bosco

## **Department of Chemistry, University of Turin, Italy**

Prof. Gianmario Martra, Dr. Yuriy Sakhno

## **Department of Medical Sciences, University of Piemonte Orientale, Novara, Italy**

Prof. Maria Prat

## **CIRIMAT Carnot Institute, University of Toulouse, France**

Dr. Christophe Drouet, Dr. Stephanie Sarda

## Fundings

**Smart nanostructured devices hierarchically assembled by biomineralization processes (SMILEY) FP7-NMP-2012-SMALL-6-310637**

**Flagship Project NanoMAX (PNR-CNR 2011-2013)**

**PNR-CNR Aging Program 2012-2014**

